TÉCNICO LISBOA

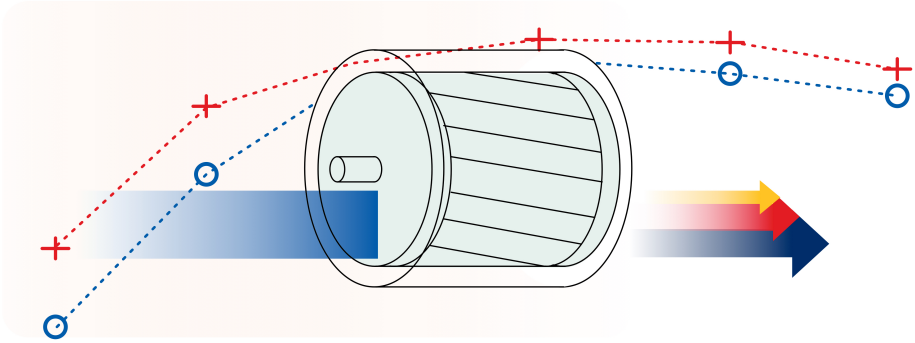

Efficiency Estimation Methods for Electric Drives using Squirrel-Cage Induction Motors

Carolina Sofia Garcias dos Santos

Thesis to obtain the Master of Science Degree in

Electrical and Computer Engineering

Supervisor(s): Prof. Paulo José da Costa Branco
MSc. Francisco Ferreira da Silva

Examination Committee

Chairperson: Prof. Célia Maria Santos Cardoso de Jesus
Supervisor: Prof. Paulo José da Costa Branco
Member of the Committee: Prof. Silviano Francisco Santos Rafael

January 2021

Declaration

I declare that this document is an original work of my own authorship and that it fulfills all the requirements of the Code of Conduct and Good Practices of the Universidade de Lisboa.

Dedicated to my friends, family and cat.

Acknowledgments

This year I had the opportunity to meet and work with incredible students, investigators and professors from the Electrical Machinery Laboratory. I want to thank Prof. Paulo Branco for showing me what a real professor is, an excellent professional and a caring and funny human being. I am immensely grateful to Francisco da Silva, who was my biggest mentor and endured hours of my questions and outbursts. You are an inspiration and a friend. A big thank you to the rest of the team from the lab, who made work become fun and colleagues become family.

A special thank you to my friend Joel, who puts up with me since the first year of college and has been my technical and emotional support since then, that never left my side in the hardest of times and always cheers me up singing ”The Final Countdown” before every exam. Thank you also to my dear friend João, who is sitting by my side while I write and always has been for this past months. You were the brightness of my days. I am deeply grateful that our paths have crossed and to be able to discover the 4th dimension trough your eyes.

Finally, the most loving thank you to my family, the ones who never let me down and are always there to bring me fresh coffee and a shoulder to cry. A small thank you to my cat, who stepped on my keyboard on a daily basis forcing me to take the break I needed. It would not be the same without you all.

Resumo

Apresenta-se um estudo sobre estimação da eficiência de uma máquina de indução num ambiente industrial usando métodos pouco intrusivos.

A precisão e o nível de intrusão dependem das medições e testes necessários. Os métodos estudados baseiam-se: no circuito equivalente, calculando todos os seus parâmetros; na segregação de perdas, associada ao princípio de funcionamento e construção da máquina; no torque, que calcula a potência de saída através da velocidade e binário; na corrente, que considera a relação da corrente de carga medida com a percentagem de carga; o escorregamento, que relaciona a razão entre o escorregamento medido e o escorregamento em plena carga com a percentagem de carga; a placa de identificação, necessitando apenas dos dados de placa.

Os diversos métodos de estimação da eficiência são aplicados a duas máquinas de indução, uma com 2,2kW e outra com 5,5kW. Os resultados são comparados com a eficiência real, em que os métodos com maior intrusividade apresentam maior precisão, assim como os testados na máquina com maior potência.

Palavras-chave: máquina de indução, estimação de eficiência,estimação de eficiência em máquinas em serviço

Abstract

This thesis presents a study on the online in-service estimation of the efficiency of an induction machine. The purpose is to be capable of measuring the efficiency in an industrial environment with non intrusive methods.

A recap on the main efficiency estimations methods is done and tested. The methods accuracy and intrusion level are dependent on the readings and tests required. The methods studied are based on: the equivalent circuit, calculating all of its parameters; the segregation of losses, which is associated with the induction machine working principle and construction; the torque, that calculates the output power with speed and torque; the input current, which considers the relation of the load current with the percentage of load; the slip, which relates the ratio of the measured slip to the full-load slip with the percentage of load, and finally the nameplate, the less intrusive methods where the only readings required are the data from the nameplate.

The several efficiency estimation methods are applied to two induction machines, one with 2.2 kW and the other with 5.5 kW. The results are compared to real efficiency, in which the methods with higher intrusiveness present a higher accuracy as expected. The methods have a bigger accuracy for bigger machines, so the results obtained for the 5.5 kW are the most satisfactory. An unexpected result was the nameplate method, with errors as low as other more intrusive methods and for a wider range of load percentage.

Keywords: efficiency estimation, in-service efficiency monitoring, induction machine

Contents

Acknowledgments vi
Resumo vii
Abstract ix
List of Tables xiii
List of Figures xv

1 Introduction **1**
1.1 Motivation 1
1.2 Objectives 2
1.3 Thesis Outline 3

2 Efficiency Estimation Methods Overview **5**
2.1 Equivalent Circuit Method 7
2.2 Segregated Losses Methods 7
2.3 Torque Methods 8
2.4 Current Methods 9
2.5 Slip Methods 10
2.6 Nameplate Methods 11

3 Induction Machine **13**
3.1 Working Principle 14
3.2 Losses in the Induction Machine 16
3.3 Simplified Equivalent Circuit 18

4 Laboratory Setup **25**
4.1 Tested Induction Machines 25
4.2 Delta and star configurations 27

5 Experimental Tests and Results **29**
5.1 Reference Efficiency 30
5.2 Estimation Methods Results 32
5.2.1 Equivalent circuit 32
5.2.2 Method B IEEE Std.112 34

5.2.3 Current Methods 44
5.2.4 Slip Methods 46
5.2.5 Nameplate Method 48
5.2.6 Tests with connected inverter 50

6 Conclusions **53**
6.1 Achievements 54
6.2 Future Work 56

Bibliography **57**

List of Tables

3.1 Relationship between X_s and X_r depending on the machine design 22
3.2 Equivalent circuit parameters 22

5.1 Assumed values for stray-load loss 39

List of Figures

3.1 REF REF REF REF Exploded view of a squirrel cage induction machine 13
3.2 Induction machine construction 14
3.3 A three-phase power supply creates a rotating magnetic field in an induction motor 14
3.4 Squirrel cage rotor 15
3.5 The Power flow diagram of an induction motor 16
3.6 Simplified equivalent circuit of the induction machine 18
3.7 Equivalent circuit of an induction machine in the no load condition 20
3.8 Equivalent circuit of an induction machine in the blocked rotor condition 21
3.9 Simulated and real values of torque and current for IM1 23
3.10 Simulated and real values of torque and current for IM2 24

4.1 IM1 setup and nameplate 25
4.2 IM2 setup and nameplate 25
4.3 Setup configuration for the experimental tests 26
4.4 Star configuration 27
4.5 Delta configuration 28

5.1 Efficiency curve of both machines 30
5.2 DC machine with movable stator coupled to the 5.5 kW induction machine 31
5.3 IM1 Efficiency curve obtained with the equivalent circuit estimation method 32
5.4 IM2 Efficiency curve obtained with the equivalent circuit estimation method 33
5.5 Extraction of friction and windage losses for IM2 35
5.6 Extraction of friction and windage losses for IM1 36
5.7 voltage drop in the core represented in the equivalent circuit of the induction machine . . 37
5.8 Simplified circuit for the core voltage calculation 37
5.9 Core power loss interpolation for IM2 38
5.10 Stray load losses plotted against squared torque 39
5.11 Induction Machine segregated losses percentage of total loss 41
5.12 IM1 Efficiency curve obtained with Method B 42
5.13 IM2 Efficiency curve obtained with Method B 43
5.14 Current estimation method efficiency curve and absolute error for IM2 44

5.15 Current estimation method efficiency curve and absolute error for IM1 45
5.16 Slip estimation method efficiency curve and absolute error for IM1 46
5.17 Slip estimation method efficiency curve and absolute error for IM2 47
5.18 Induction Machines efficiency load curves 48
5.19 Nameplate estimation method efficiency curve and absolute error for IM1 49
5.20 Nameplate estimation method efficiency curve and absolute error for IM2 49
5.21 Efficiency curves for IM1 with and without a connected inverter 50
5.22 Voltage and current waveforms of the induction machine with and without a connected inverter 51
5.23 Efficiency estimation methods results for an inverter fed induction machine 51

6.1 Efficiency estimation methods comparison 55

Chapter 1

Introduction

1.1 Motivation

The consumption of electricity by induction motors in the industrial sector accounts for approximately 2/3 of the total electricity consumed. Therefore, this is a huge matter of study considering the current energetic problem in the world. It's of major importance to try to minimize the world's resource consumption and to have efficient machines working in the industry.

For this reason, there is the need for sophisticated and precise methods of measuring the motor's efficiency in order to replace the inefficient machines by efficient ones. Since induction machines are the most used machinery in industrial applications, this was the type of machine chosen to perform all the experimental tests.

The IEEE standard test procedure [1] describes several methods for determining the performance characteristic of polyphase motors. These methods involve tests with no load, with variable load, with the rotor blocked and even with the rotor taken out, among other types of tests. In an industry context, all this tests would interfere with the machine's usual performance during a working day or routine. This intrusive tests are very accurate, and usually the more intrusive they are, the more accurate are the efficiency results. Although the accuracy is high, this level of intrusiveness would disrupt the production process of the power plant and decrease profit. In a real power plant, this tests are not feasible, for example, in many cases it is not possible to decouple the motor from its original load and that would imply to much installation costs and time. Thus it is necessary that these methods are as less intrusive as possible so there's no need for stopping or compromising the machine's performance in order to measure its efficiency.

This way, instead of directly measuring the losses or the output power, it is possible to estimate them. With less intrusive estimation methods, an estimation of the motor efficiency can be obtained during its working routine (in-service), although with reduced accuracy. This estimations are based on mathematical models of the motor and tend to use just line currents and voltages that can be taken online.

1.2 Objectives

The main purpose of this study is not only to technically expose several methods of estimating the efficiency of an induction machine, but also to understand its meaning and to sensitize the reader for the enormous variables at stake when trying to estimate the efficiency of a machine. Understanding the equations and the working principle of the machine, as well as the physical quantities that can be measured, one can combine several existing methods in order to suit the existing conditions and restrictions of the application needed.

For that, the objectives purposed and accomplished are to:

- Recap the main efficiency estimation methods, focusing on the ones that sustain the basis of all the methods, namely the equivalent circuit methods, segregated loss methods, torque methods, current methods and slip methods.
- Test how the results vary depending on the variables needed and present a possibility for the reader to decide on how much intrusiveness is worth increasing in change of accuracy
- Accompany the experimental tests with a theoretical component on the induction machine characteristics and working principle in order to give the reader tools to explore further more complex methods that suit the specific requirements of each application.

1.3 Thesis Outline

There are plenty of efficiency estimation methods, from standards of entities like IEEE and IEC to methods created by companies or institutes that are not so easily available. In the Chapter 2, the main estimation methods are presented briefly before choosing the ones that will be tested.

Because the efficiency of a machine has everything to do with its construction and working principle, this two topics are discussed in Chapter 3, explaining all the machine components and its associated losses. The equivalent circuit is introduced and its parameters are calculated in order to obtain the steady state characteristic of the induction machine. The no load and blocked rotor test needed to estimate the equivalent circuit parameters are also included in this chapter.

In Chapter 4, the machines used in the experimental tests are introduced as well as the configurations of the two setups used for the testing: with and without an inverter feeding the induction machine. Since that an important part of estimating the efficiency is the ability to measure the respective variables and quantities needed, a small note on the variations of this readings depending on the configuration of the machine is emphasized in this chapter.

The tests and procedures of the methods experimental tested are enumerated in Chapter 5 and its results are presented. A reference efficiency is calculated and the comparison of the accuracy of the different estimation methods is based on the absolute error between the estimation and the reference efficiency curve.

The final conclusions in Chapter 6 take into account the differences between the several methods, and do a balance on their advantages and drawbacks pondering the accuracy versus the intrusion level.

Chapter 2

Efficiency Estimation Methods Overview

The main focus of this thesis is to study ways to estimate the efficiency of an in-service induction machine. In this chapter, the main methods are presented and introduced.

Efficiency in (2) is defined as the ratio between the input power P_{In} and the output power P_{Out} of a machine.

$$\eta = \frac{P_{Out}}{P_{In}} \times 100 \tag{2.1}$$

This is a direct method to calculate the efficiency of the induction machine. Both the output power and the input power can be measured reasonably well with transducers and appropriate measuring instruments [2]. The output power can be calculated from the product of torque and angular velocity.

The efficiency can also be calculated by indirect methods, that is, methods that calculate the output power by obtaining the machine losses and subtracting them to the input power,

$$\eta = \frac{P_{In} - P_{Losses}}{P_{In}} \times 100. \tag{2.2}$$

For this, the machine losses are calculated individually, segregated, and are obtained through several tests. These two methods are very accurate but usually, in an industrial environment, there may not be any sensors installed in order to measure torque or it might not be possible to take the machine out of service in order to perform all the tests needed for the segregated loss method.

Hence instead of actually measuring the output power or the losses of the machine, it is possible to estimate them with non-intrusive in-service motor efficiency estimation methods, which are able to estimate the efficiency of the motor while operating and without compromising its usual performance. This methods are typically based on a mathematical model or equivalent circuit of the machine and use the information of the nameplate or the line current and voltage to perform its estimation.

These estimation methods are classified according to their level of intrusion [3], which depends on the data parameters needed to calculate the efficiency. If the method only requires data from the nameplate to calculate the efficiency, than the intrusion level is very low, but the accuracy might not

be the highest. Whereas if another method requires a test with the machine stopped or with the rotor blocked, the intrusion level is high and not all machines can be taken out of service, yet the accuracy of the readings can also be higher.

Therefore, in this chapter, the main methods for estimating the efficiency of an induction machine are introduced in a decreasing order of intrusiveness. The methods presented are divided in Equivalent-circuit methods, which simplify the induction machine characteristics in a mathematical model and the Segregated Losses methods, which are the ones recommended by most standards as an accurate indirect method for the type of machines studied. The Torque methods, which calculate the mechanical power through torque and also Slip and Current methods, that use speed and current readings respectively to estimate an approximate value of the efficiency. These several types of methods can also be combined in order to achieve a better accuracy [4]. The best method for each application should be chosen considering both the level of intrusion that is possible and the level of precision that is needed.

2.1 Equivalent Circuit Method

It is possible to estimate the efficiency of the induction motor based on its equivalent circuit. This way the efficiency can be estimated for operating points and conditions rather than those at which measurements are made. The standard equivalent circuit method is presented by IEEE [1] and is the basis for the further modified and less intrusive methods. There are several equivalent circuit methods and above are summarized the two most accurate and non intrusive, since the others are too impractical to be applied in an industrial motor.

The *Nameplate Equivalent-Circuit (ORMEL96) Method* is obtained from the nameplate data and the stator resistance. The stray load losses are represented by a parasitic resistance inserted in the rotor and the stator resistance can be estimated from nameplate data. The parameters of the equivalent circuit are solved from an assumed rated load condition and locked rotor condition, which completely rely on motor nameplate information and may have up to 20% inaccuracies according to NEMA [3] [5].

Another equivalent circuit method is the *Rockwell Motor-Efficiency Wizard (RMEW) Method*, which relies on measuring the input current, the input electrical power, the stator resistance and the output speed of the motor [6]. The stator resistance can be measured at a certain temperature and then be estimated for different temperatures. The other parameters of the equivalent circuit can be measured using two operating points.

2.2 Segregated Losses Methods

As the name suggests, these methods separate and estimate each one of the losses presented in section 3.2 and subtract them to the input value.

The IEEE Standard Test Procedure for Polyphase Induction Motors and Generators [1] states that horizontal machines rated at 0.7457 kW to 300 kW should be tested using Efficiency Test Method B, the input-output method with loss segregation. This method is less intrusive than the Equivalent circuit method because the locked rotor test is not required, but still has a high level of intrusion, although very accurate.

Between several methods of this type, the most suitable for the in-service efficiency estimation is the Ontario Hydro Modified Method E (OHME). This is an improved version of the IEEE Std-112 method E1 [1], which assumes a value for the stray load losses at a rated load depending on the motors size. In the OHME method the windage, friction, and core losses are combined and assumed to vary between 3.5%–4.2% of rated input power [7], making the no-load test not required. Once more, this assumptions degrade the accuracy of the results but decrease its intrusiveness.

2.3 Torque Methods

The basis for all the torque methods is that the output power of a motor is the product of the shaft angular speed and shaft output torque.

Knowing the shaft torque T_{shaft} and measuring or estimating the rotor speed ω_r and the input power P_{In}, it is possible to calculate the efficiency following (2.3).

$$\eta = \frac{T_{shaft}\omega_r}{P_{In}} \tag{2.3}$$

This output torque is the air-gap torque T_g subtracted by the torque losses,$P_{fw} + P_{SL}$, associated with friction, windage, and stray losses caused by rotor currents, respectively. (2.3) is then equivalent to

$$\eta = \frac{T_g\omega_r - P_{fw} - P_{SL}}{P_{In}}. \tag{2.4}$$

The Air-Gap Torque (AGT) Method calculates the air-gap torque with line currents and voltages. The torque derivation takes into account the unbalanced supply, which reflects the industrial plants reality, and can be measured online, which is financially appealing for industries that cannot afford stopping its machines. However, the losses have to be measured with the no load test, representing the main drawback of this method for its high intrusion level.

The Shaft Torque Method measures the output power ($T_{shaft}\omega_r$) directly from the shaft using torque transducers. However, this method is too expensive and highly intrusive.

The method used to calculate the reference efficiency is a torque method based on the the calculation of the torque coefficient K of the DC machine, coupled to the induction machine, and is explained in section 5.1.

2.4 Current Methods

The current methods provide a higher accuracy when compared to the slip methods. Both are based on nameplate parameters and in the *Standard Current Method*, it is assumed that load current varies linearly with the percentage of load.

$$\eta = \frac{I}{I_{\text{rated}}} \cdot \frac{P_{\text{output, ratod}}}{P_{\text{input}}} \tag{2.5}$$

This method results in errors due to the actual non linearity of the load curve and tends to overestimate the efficiency curve. As in the slip methods, the manufacturer parameters are not reliable when there's the need for high precision, since by NEMA [5] the current should not vary by more than 10% of the nameplate current.

The advantage of this current based method is its simplicity and non intrusiveness. In order to improve its accuracy it is possible to add the no load current to the formula given by (2.6), yet it would be more intrusive to measure it.

$$\eta = \frac{I - I_{no_load}}{I_{rated} - I_{noload}} \frac{P_{outputrated}}{P_{input}} \tag{2.6}$$

This method, on the other hand underestimates the efficiency, so an average of the two usually gives a better result.

2.5 Slip Methods

This type of methods are based on the assumption that the ratio of the measured slip to the full-load slip is proportional to the percentage of load. *Standard Slip Method* is a simple method, which uses the measurements of the speed to find the slip, which is usually a reading with low intrusiveness. The input power has also to be measured, being it a more intrusive procedure. The efficiency is then approximated by (2.7).

$$\eta = \frac{s}{s_{rated}} \frac{P_{outputrated}}{P_{input}} \tag{2.7}$$

The obvious error is that the slip ratio represents the percentage of load and the efficiency is not equal to the percentage of load [8].

The previous method can be improved by correcting the rated nameplate speed for voltage variations in the *Ontario Hydro Modified Slip Method* given by

$$\eta = \frac{s}{s_{rated}} \frac{P_{outputrated}}{P_{input}} \left(\frac{V}{V_{rated}} \right)^2 . \tag{2.8}$$

Although this methods are an improvement of a merely nameplate based efficiency estimation method, it still uses nameplate data. According to NEMA MG-1 Section 12.46 [5] the variation from the nameplate speed of AC integral horsepower induction motors shall not exceed 20% of the difference between synchronous speed and rated speed when measured at rated voltage, frequency, and load and with an ambient temperature of 25ºC. Also the voltage will not always be the rated one in which the values of the nameplate were measured.

These slip methods can still be improved by measuring the current and the stator resistance ,

$$\eta = (1 - s) \left(\frac{3 I_{Load}^2 R_s}{P_{Load}} \right) \tag{2.9}$$

2.6 Nameplate Methods

The methods that use motor information from the nameplate data are naturally the least intrusive methods, since there is only the need to access the motor's nameplate. An example of an induction motor nameplate is shown in figure 4.1a.

In the *Standard Nameplate Method* efficiency is assumed to be constant and equal to the value in the nameplate [7]. Therefore, this method has greater accuracy in cases where the efficiency-load curve is reasonably flat so that the value of efficiency in the nameplate, correspondent to full load, is suitable for a large range of load percentage. Hence, this method can have a large error in accuracy when applied to certain types of motors with non flat curves.

Also, the field environment may be different from the one used to acquire the nameplate data values, which influences the voltage unbalance and the harmonics content. Additionally, the nameplate data is no longer valid for rewound motors, although there is the opinion that if the rewound follows the *Electrical Apparatus Service Association (EASA)* standard procedures, the efficiency is not reduced [7].

Another disadvantage of these methods is that there are a couple of different standards for efficiency tests and measurement procedures, which leads to discrepancies in the adopted testing standards when nameplating the efficiency [9].

A variation of the previous method is the *Volgelsang and Benning (V & B) Method* with two different options, the first requires tests with no load, normal load and unpowered while the second uses Nameplate data.

Chapter 3

Induction Machine

Induction machines are the most common electrical machines for industrial applications. Their easy maintenance, simple installation and control, adding to its low cost and high efficiency make them very popular around the world. They are asynchronous machines in which the electric current is induced in the rotor by a rotating magnetic field created by the alternated current flowing through the windings of the stator. A squirrel cage induction machine is shown in figure 3.1.

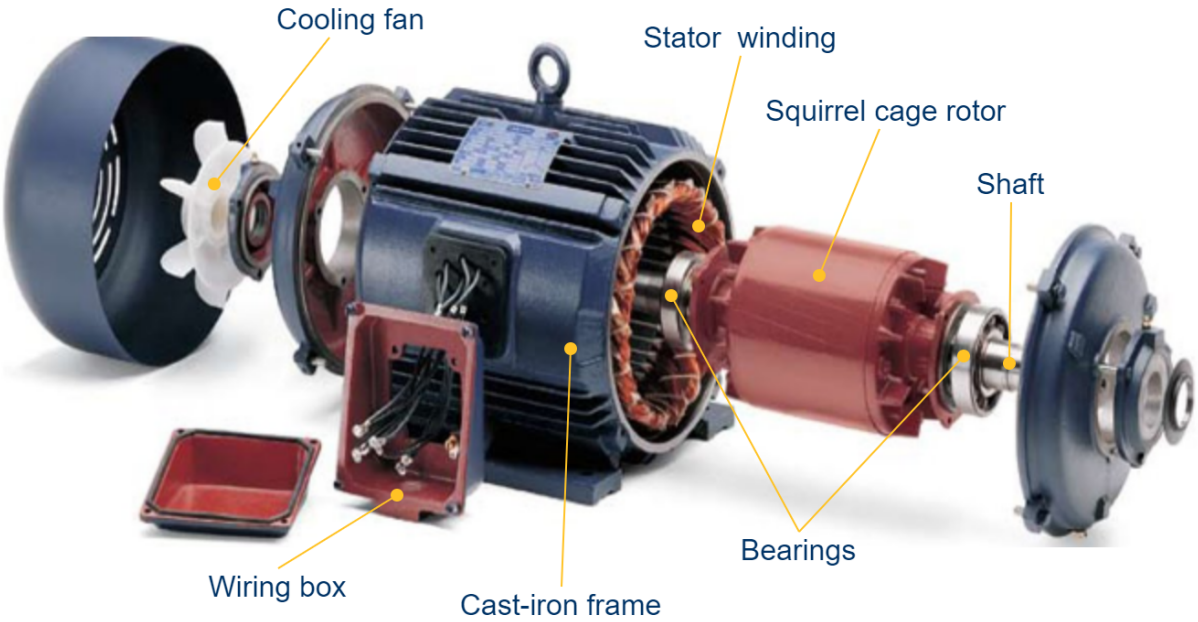

Figure 3.1: REF REF REF REF Exploded view of a squirrel cage induction machine

In this chapter, the several parts of the induction machine are presented, as well as their role in the working principle. After understanding the induction machine construction and operation, it is intuitive to see where the power can get dissipated and the machine's losses are explained. In order to represent the machine in a mathematical model, the equivalent circuit is introduced, which is also useful to calculate some losses in the estimation methods.

3.1 Working Principle

The induction machine is made of two main parts: the stator and the rotor in figure 3.2.

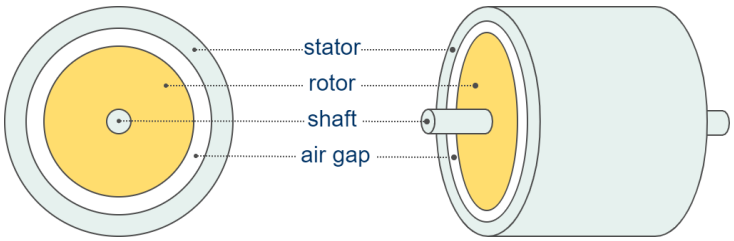

Figure 3.2: Induction machine construction

In this motor, the time-changing current in the stator creates a magnetic field that induces current in the rotor. This way, the stator consists of an iron core with slots, where a three phase winding is electrically placed 120º apart. The machines studied are three phase machines, but there are also single phase induction machines, for example.

This three phase current flowing through the stator windings creates a magnetic field, exemplified in figure 3.3. Since the current is changing, the magnetic field is also changing, it rotates in synchronism with the AC oscillations at a velocity called the synchronous speed N_s. The synchronous speed N_s depends on the electrical frequency of the stator f_s, on the number of pairs of poles pp of the machine and can be calculated by

$$N_s = \frac{120 f_s}{pp}. \tag{3.1}$$

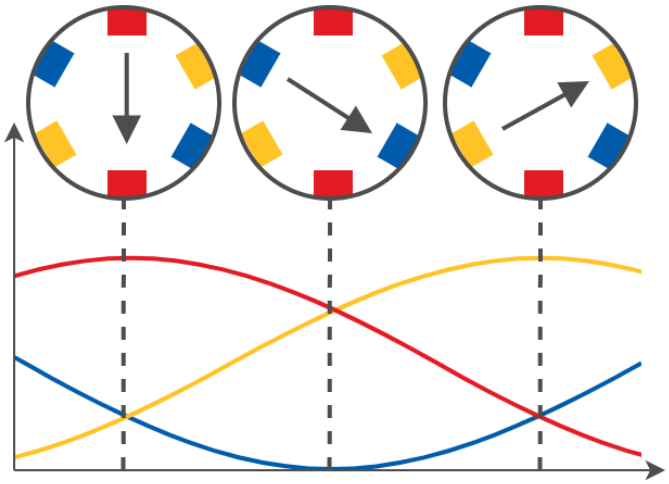

Figure 3.3: A three-phase power supply creates a rotating magnetic field in an induction motor

As seen in figure 3.1 and 3.2, the rotor is suspended inside the stator and therefore, within its magnetic field. The rotor in figure 3.4 consists of several copper conductor bars, short circuited at both sides by end rings. This structure is also placed inside a laminated iron core to avoid losses from eddy currents. The conductor bars of the squirrel cage rotor are skewed since this increases the transformation ratio and prevents cogging during the starting process.

According to Faraday's law, the sator magnetic field rotation induces an EMF in the conductor bars

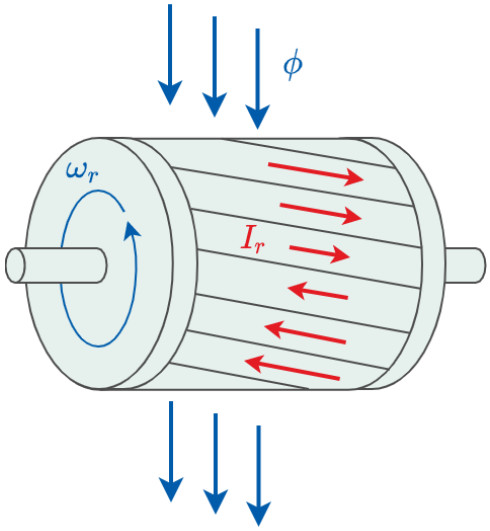

Figure 3.4: Squirrel cage rotor

and since they are short circuited, the EMF creates eddy currents flowing trough the rotor bars in loops. Once more, this currents create a magnetic field, which interacts with the stator magnetic field.

Lenz's law of electromagnetic induction states that, when an EMF is induced according to Faraday's law, the direction of that induced EMF is such that it opposes the cause of its production. Therefore, the direction of the current in the rotor is such that the magnetic field created by it opposes the initial changing stator magnetic field. This way, to oppose the changing current in the rotor bars, a force is induced on them, the Lorentz force, and the rotor starts to rotate. The direction of rotation is the same as the stator magnetic field, acting in an effort to eliminate the difference in motion between them. Since the rotor is fixed with bearings, the forces created in the rotor produce an electromagnetic torque.

For the current to be induced in the rotor, the rotor's speed must be different from the synchronous speed. For this reason, the induction machine is also called Asynchronous machine, since the speed N of the rotor does not reach the synchronous speed N_s.

When the induction machine is working as a motor, the rotor speed is lower than the speed of the stator magnetic field and their relative difference is called slip s, which is written as

$$\mathrm{s} = \frac{(n_s - n)}{n_s} \,. \tag{3.2}$$

3.2 Losses in the Induction Machine

From the moment that a three phase power P_{In} enters the stator of the machine to its transformation in mechanical output power P_{Out}, there are losses that occur in several stages of this process. The power flow of the induction motor is diagrammatized in figure 3.5.

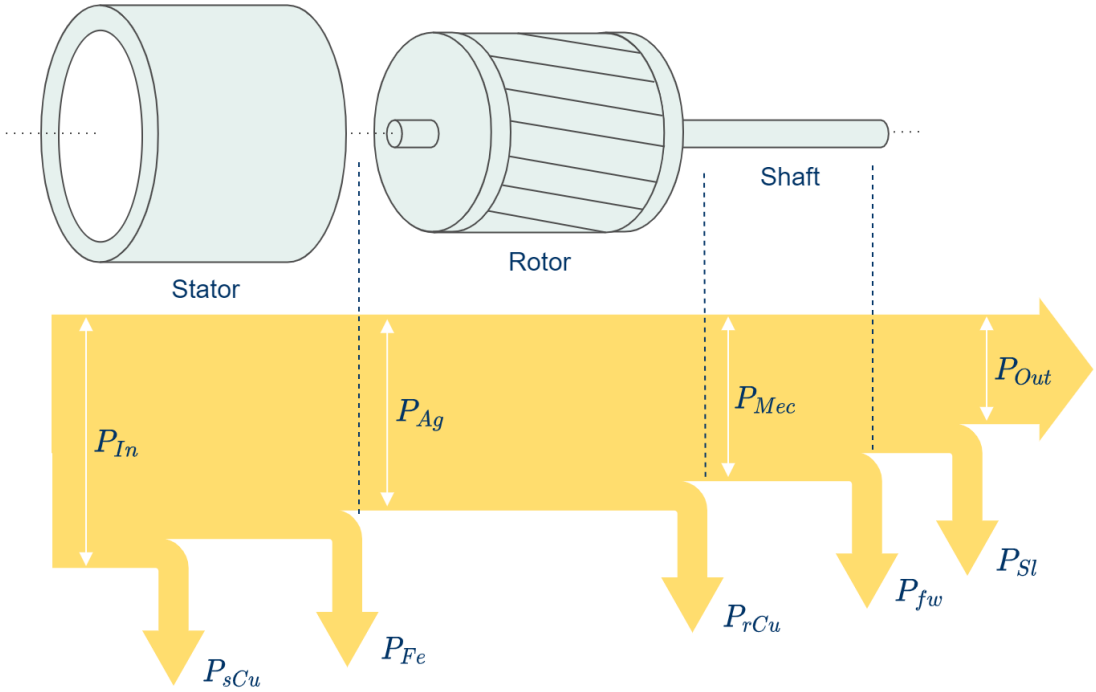

Figure 3.5: The Power flow diagram of an induction motor

When the three phase current flows through the stator copper windings, some power is lost as heat by Joule effect. This loss is called stator copper loss or stator joule loss P_{sCu}.

This flowing current creates a changing magnetic field which is responsible for the core loss. The core loss or iron loss P_{Fe} consists of hysteresis loss, eddy current loss, and excess loss. Hysteresis loss is due to the magnetic material experiencing cyclic variations caused by the rotating magnetic flux. Also because of the alternating fluxes, eddy currents circulate in the iron core. This process generates heat, that is, eddy currents loss. This is why, to reduce eddy currents, the stator and rotor core are laminated. The excess loss is due to the nonuniform distribution of magnetic flux, created by its nonlinear diffusions and skin effect [10]. Subtracting these losses from the input power P_{In}, the power in the air gap P_{Ag} is obtained. This power than goes to the rotor.

In the same way, there are copper joule losses in the rotor P_{rCu}, due to the current flowing through the conductor bars, as well as core losses, because of the magnetic field created by those currents. The core loss depends upon frequency of the supply voltage, so while the stator frequency is equal to the supply frequency f, the rotor frequency is the slip times the supply frequency $(s \times f)$. That is, if the frequency of the supply is 50Hz, which is the case, the rotor frequency is between 2% to 5% the stator frequency, which would be around 1Hz to 2.5Hz. Thus the rotor core loss is neglected, since it is too small compared to the stator core loss.

Besides ohmic loss in the conductors and magnetic loss in the laminations, there are also mechanical

losses due to friction and windage P_{fw}. The power P_{Mec} that the rotor produces is still not the output power and has losses due to its movement. This losses are unavoidable in a rotational machine. If a machine rotates there is power being lost due to friction in the bearings, which can be modeled by the Couloumb friction model [11]. When the shaft rotates, it displaces air. The power lost to air friction is called windage loss.

Finally, the stray load losses are the most unknown element of the balance of power in induction machines [12]. This loss lumps all of the electromagnetic losses which occur because the machine does not have a smooth air gap and sinusoidal winding distributions [11]. Following several standards, the stray-load loss is considered to be the portion not accounted for the sum of the losses mentioned above.

The power left after taking all the losses is the output power P_{Out} and is the actual useful power produced by the machine. In an induction machine, the output power is usually between 85% and 95% of the input power. These percentages are actually the efficiency of the machine, so the calculation of losses is directly related to finding the efficiency of a machine and are used in several efficiency estimation methods.

3.3 Simplified Equivalent Circuit

In order to simplify the study of the induction machine steady state behaviour, the system is represented by means of an equivalent circuit. The equivalent circuit represents only one stator phase and is useful for predicting the currents, output power and torque of the motor. The calculations needed to reach this model are fully explained in [13]. This circuit in figure 3.6 represents the three main parts of the construction of the machine: the stator, the rotor and the magnetic core. The parameters of the equivalent

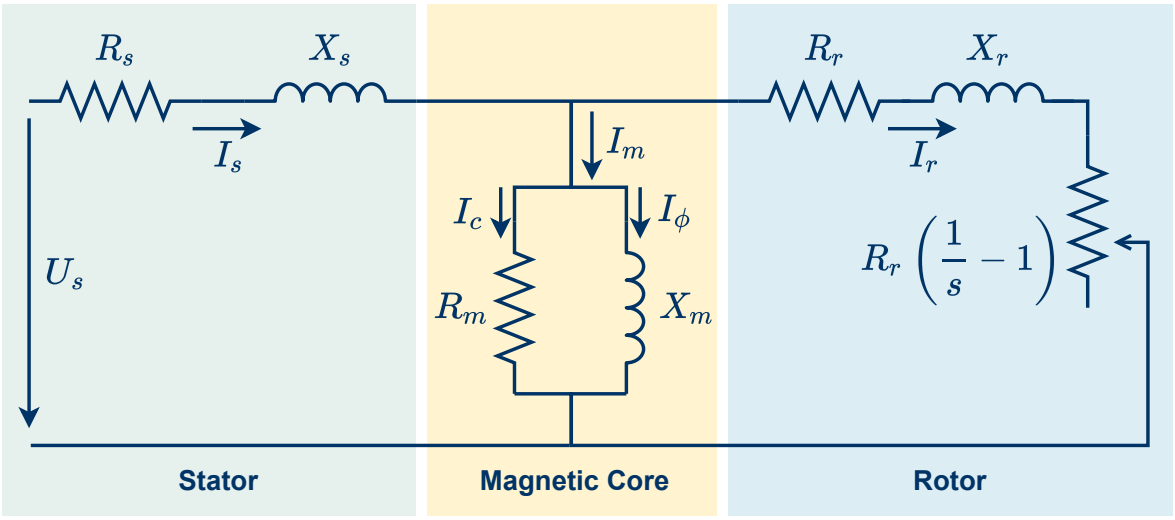

Figure 3.6: Simplified equivalent circuit of the induction machine

circuit are:

- X_s - field leakage reactance in the stator
- X_r - field leakage reactance in the rotor
- X_m - magnetic reactance responsible for the rotating magnetic field in the air-gap
- R_s - stator resistance representing the joule loss in the stator
- R_r - rotor resistance representing the joule loss in the rotor
- R_m - core resistance representing the joule loss in the core

The left side of the circuit represents the stator, where the stator joule losses are accounted by the resistance R_s, and the field leakage is represented by the reactance X_s. the right side of the circuit represents the referred rotor resistance R_r and rotor leakage reactance X_r at slip frequency. The stator current $\overline{I}_s$ is divided into an exciting component $\overline{I}_m$ and a load component $\overline{I}_r$ that corresponds to the mmf of the rotor current. The losses correspondent to the excitation are represented by the magnetizing branch with the core loss resistance R_m which represents the joule losses in the core and the magnetizing reactance X_m in parallel, responsible for creating the rotating magnetic field in the air-gap. The combined effect of the shaft load and rotor resistance appears as a reflected resistance $R_r\frac{1-s}{s}$, a function of slip and therefore of the mechanical load. The power delivered to this component

is equivalent to the electromechanical power per stator phase [13]. If the parameters of the circuit are known, it is possible to know the steady state characteristics of the machine.

As seen in section 3.1, the induction machine has several types of losses associated with its materials and rotational movement. Some of the losses can be calculated from the parameters of the equivalent circuit, since it models the induction machine.

In order to obtain the parameters of the equivalent circuit, two tests are performed: the no load and the blocked rotor test. In the no load test, since the motor is ran with no connected load, it is possible to obtain the parameters relative to the constant losses, the ones that do not depend on the load point. The copper joule losses, dependent on the amount of current flowing in the stator and rotor winding, can be obtained from the blocked rotor test.

In this section, it is explained how the parameters of the equivalent circuit were obtained and why some approximations were considered. The losses referred in this section are explained in detail in section 3.2.

No load

With the motor running with no connected load, there is no useful work being done, except the one needed to overcome the rotor's inertia and make it rotate. This way, there are two processes draining power from the machine. First, are the losses involved with the process of creating the rotating magnetic field, the one responsible for inducing current in the rotor. These are the core or iron losses. The second one, is the power needed to overcome the friction and windage losses associated with the rotating movement of the rotor. Both of these losses are considered constant for the normal operation of the machine.

For the estimation of the parameters, the following readings are needed

- P_{nl} - no load stator input power
- V_{nl} - no load phase stator voltage
- I_{nl} - no load phase stator current
- $cos(\phi)$ - power factor

The measurements and calculations presented refer to a star connected machine. For a delta connected machine, the changes needed can be found in section 4.2.

Given that the majority of input power consumed by the machine goes to its losses, the output power is almost null, so the current in the rotor is very small. In addition to the losses related to the rotational movement, there are also copper joule losses in the stator P_{sCu}, which are not constant and are calculated as follows,

$$P_{sCu} = 3I_{nl}^2 R_s. \tag{3.3}$$

The measurement of resistance R_s can be done directly and is explained in section 4.2. The parameters of the equivalent circuit in this section correspond to a stator resistance measured during the rated load test in 5.2.2.

The rest of the power consumed is due to core loss P_{Fe} and mechanical losses from windage and friction P_{fw}:

$$P_{nl} - P_{sCu} = P_{Fe} + P_{fw}. \tag{3.4}$$

Having no load, the rotor will rotate at nearly synchronous speed N_s,

$$N \approx N_s \tag{3.5}$$

which makes the slip s nearly zero

$$s = \frac{N_s - N}{N_s} \xrightarrow[N \to N_s]{} 0. \tag{3.6}$$

This way, it can be assumed that the current in the magnetic branch I_m is approximately the amount of current entering the stator I_{nl}, since the parameter $R_r(\frac{1}{s} - 1)$ is so high that it is considered an open circuit. The equivalent circuit in this condition is approximated as depicted in figure 3.7.

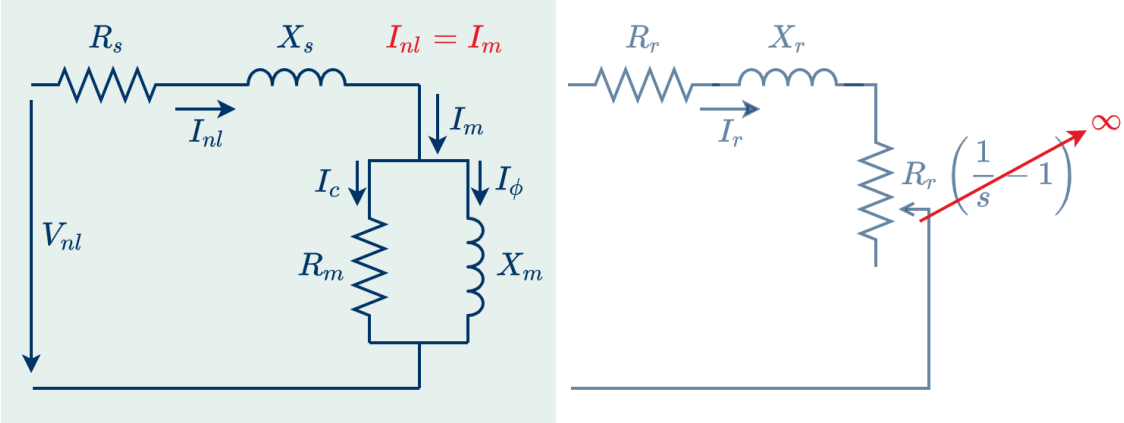

Figure 3.7: Equivalent circuit of an induction machine in the no load condition

From the new equivalent circuit, the core loss current I_c and the magnetizing current I_ϕ are obtained by dividing the excitation current $I_m = I_{nl}$ in its resistive and inductive component, as follows

$$I_\phi = I_{nl} sin(\phi) \tag{3.7}$$

$$I_c = I_{nl} cos(\phi). \tag{3.8}$$

Given that $X_s << X_m$, the reactance X_m is then easily calculated from I_ϕ, V_{nl} and rated frequency $f = 50$ Hz:

$$L_m = \frac{V_{nl}}{2\pi f I_\phi} \tag{3.9}$$

$$X_m = 2\pi f L_m \tag{3.10}$$

The drop voltage in the resistance R_s could be neglected, being it much smaller than V_{nl}, but since it is easily measured, its value is considered for the calculation of resistance R_m,

$$R_m = \frac{V_{nl} - I_{nl} R_s}{I_c}. \tag{3.11}$$

Blocked Rotor

The blocked rotor test is used to obtain the parameters relative to the stator and rotor branches, namely the rotor resistance R_r and the reactance of the sator X_s and rotor X_r. In this condition, the rotor is physically prevented from rotating and a reduced voltage is applied to the stator, so that there is rated current in the stator winding. The speed of the rotor is $N = 0$ and therefore slip $s = 1$, making the parameter $R_r(\frac{1}{s} - 1) = 0$.

In this conditions. the following quantities are measured

- P_{br} - blocked rotor stator input power
- V_{br} - blocked rotor phase stator voltage
- I_{br} - blocked rotor phase stator current
- $cos(\phi)$ - power factor

Note that, the resistance R_m is much bigger than R_r, as well as the X_m is much bigger than $X_s + X_r$, so the magnetic branch part of the circuit can be ignored. Figure 3.8 shows the simplified circuit for the blocked rotor condition. This way, the input power P_{br} is lost in the resistances R_s and R_r due to copper

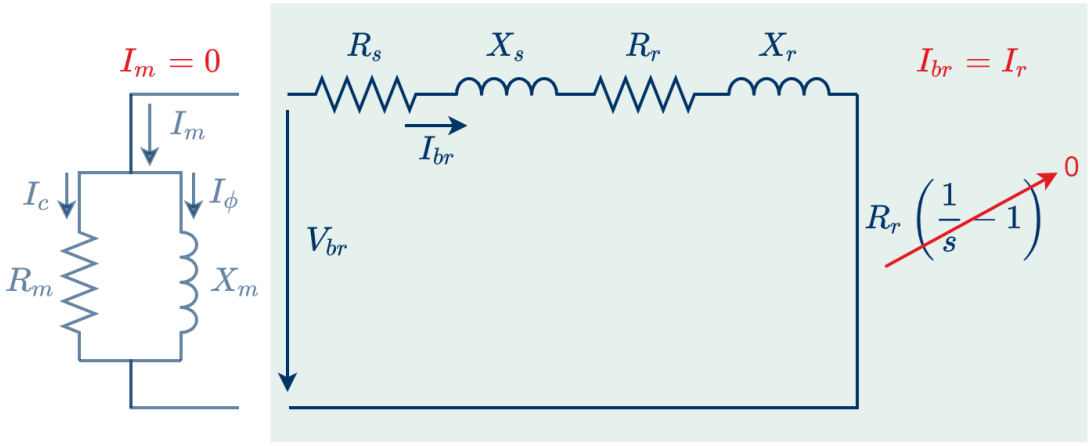

Figure 3.8: Equivalent circuit of an induction machine in the blocked rotor condition

joule losses.

In order to obtain these parameters, the equivalent impedance Z_{eq} is calculated from the stator voltage and current as follows

$$Z_{eq} = \frac{V_{br}}{I_{br}}. \tag{3.12}$$

Measuring the stator resistance R_s as in section 4.2, it is possible to calculate R_r by

$$R_r = Z_{eq}cos(\phi) - R_s \tag{3.13}$$

and the total leakage reactance X_{eq} by

$$X_{eq} = Z_{eq}sin(\phi). \tag{3.14}$$

The total leakage reactance is the sum of both stator and rotor reactances,

$$X_{eq} = X_s + X_r, \tag{3.15}$$

and the ratio $\frac{X_s}{X_r}$ varies depending on the design of the machine. This classification is defined in NEMA MG-1 [5] and is based on the starting characteristics of the machine.

Table 3.1 gives the ratio assumed for each design according to IEEE std-112 [1]. The ratio used is the one relative to the design B.

Machine design	X_s/X_r
A	1
B	0.67
C	0.43
D	1

Table 3.1: Relationship between X_s and X_r depending on the machine design

The parameters of the equivalent circuit are calculated and can be seen in table 3.2.

Machine	IM1	IM2
$R_r[\Omega]$	1.88	0.94
$X_r[\Omega]$	5.11	3.86
$X_s[\Omega]$	3.40	2.57
$R_m[\Omega]$	11820	652
$X_m[\Omega]$	64.42	87.2

Table 3.2: Equivalent circuit parameters

With the parameters obtained, it is possible to calculate the steady-state characteristics of the machine.

The stator impedance Z_s is the sum of the resistance and reactance of the stator branch,

$$Z_s = R_s + jX_s \tag{3.16}$$

the rotor impedance Z_r, in the same way is,

$$Z_r = \frac{R_r}{s} + jX_r \tag{3.17}$$

and the magnetizing impedance Z_m is the parallel of the magnetizing branch parameters

$$Z_m = \frac{jR_cX_m}{R_c + jX_m}. \tag{3.18}$$

This way, the equivalent thevenin impedance is

$$Z_{eq} = Z_s + \frac{Z_m\, Z_r}{Z_m + Z_r}. \tag{3.19}$$

From the thevenin equivalent, the equivalent stator voltage V_{seq} when the rotor circuit is removed is

calculated as follows

$$V_{seq} = V_s \frac{Z_m}{Z_m + Z_s}. \tag{3.20}$$

From the equivalent thevenin circuit, the current in the rotor $\overline{I_r}$ is

$$\overline{I_r} = \frac{V_{seq}}{Z_s + Z_r} \tag{3.21}$$

so the mechanical power P_{mec} is equal to

$$P_{mec} = 3I_r^2 \frac{R_r}{s}. \tag{3.22}$$

This way, the torque is determined by its relation with the shaft angular speed and the mechanical output power, as seen in section 2.3,

$$T = 3I_r^2 \frac{R_s}{s}. \tag{3.23}$$

The stator current is as follows,

$$\overline{I_s} = \frac{V_s}{Z_{eq}} \tag{3.24}$$

and is plotted with torque against the speed of the rotor in figures 3.10 and 3.9. The shape of the torque curve varies depending on the rotor resistance R_r, a difference possible to observe in these figures. The pull-up torque (maximum torque value) and breakdown torque (minimum torque value) in pu of IM1 are larger than IM2. Comparing the estimated values with the real values, it is possible to see that in IM1 estimated curves, the speed and torque reach the rated values (dark blue circles) for a speed higher than the rated one (yellow circles), while the real curve is closer to the rated speed. For IM2 estimated curves, the torque and current reach the rated values for values of speed lower than the rated value, while the real curves are very close to the rated speed.

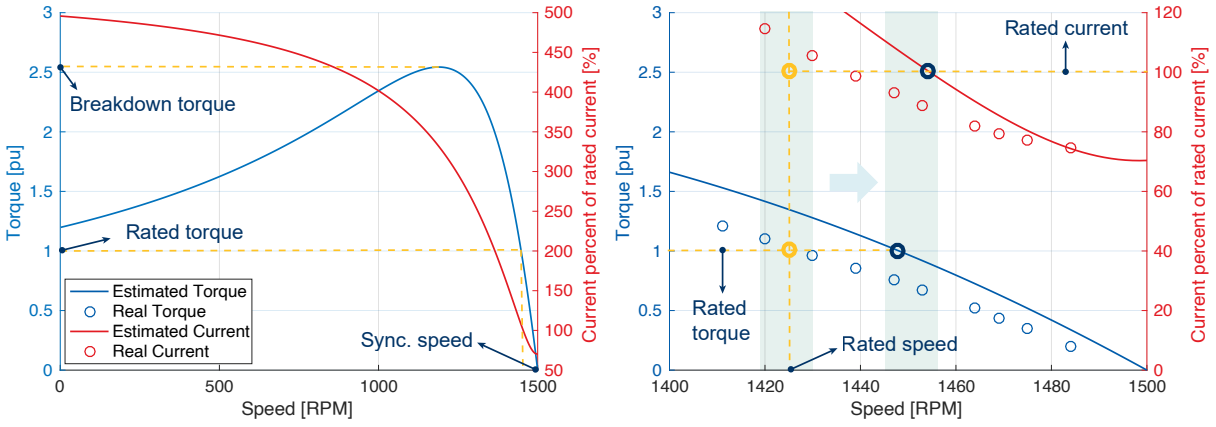

Figure 3.9: Simulated and real values of torque and current for IM1

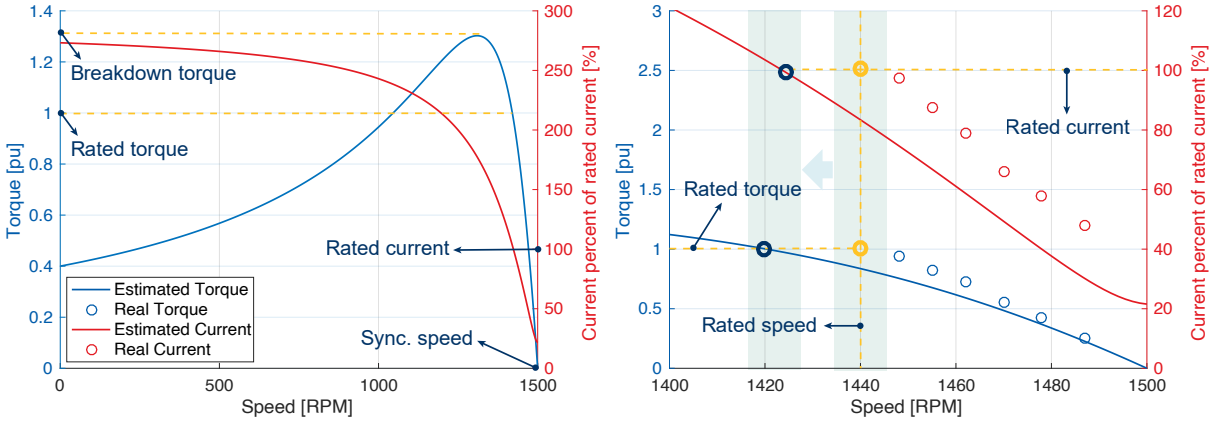

Figure 3.10: Simulated and real values of torque and current for IM2

Chapter 4

Laboratory Setup

4.1 Tested Induction Machines

In order to compare the several efficiency estimation methods, experimental tests were made in two different machines. The induction machine 1 (IM1) has 2.2 kW of rated power and is connected with a DC machine. The induction machine 2 (IM2) has 5.5 kW of rated power and is also connected to a DC machine but with a movable stator. Machines IM1 and IM2 are shown presented in figures 4.1 and 4.2, respectively, along side with their nameplates.

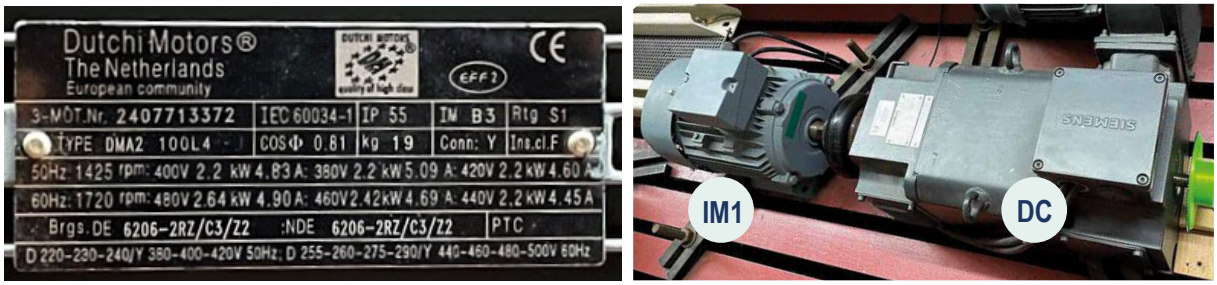

(a) Nameplate (b) IM1 coupled to a DC machine

Figure 4.1: IM1 setup and nameplate

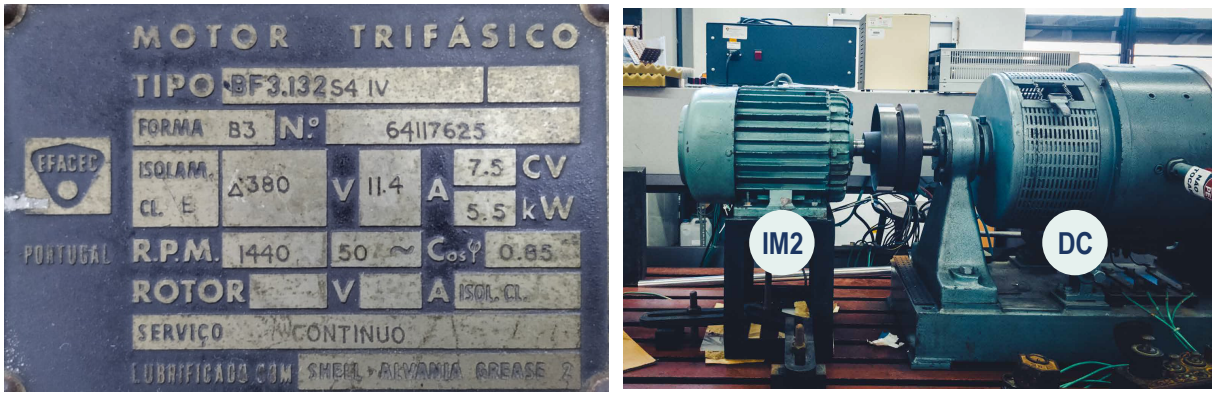

(a) Nameplate (b) IM2 coupled to a DC machine

Figure 4.2: IM2 setup and nameplate

A simplified diagram of the setup used is shown in figure 4.3. The same tests are performed with a V/f inverter (setup 2) and without it (setup 1). In setup 1, an auto-transformer regulates the voltage coming from the grid, that is used to feed the induction machine. The current source, supplies the excitation current for the DC machine and the load is simulated by a resistive bank connected to the armature of the DC machine. To acquire the measurements, the following equipment is used: current probes, multimeters and a Three-Phase Power Analyzer.

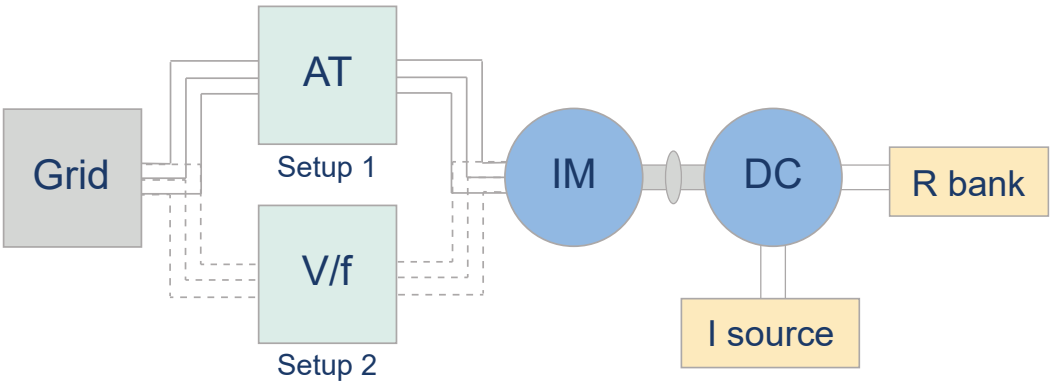

Figure 4.3: Setup configuration for the experimental tests

4.2 Delta and star configurations

The stator windings of an induction machine can be connected in two different configurations: star and delta. Usually there are 6 terminals accessible outside the machine's stator and the inside configuration of the stator windings is shown in figures 4.4 and 4.5.

The star configuration is obtained by short circuiting 3 terminals of the same side, like it is shown in figure 4.4. This way, the phase voltage V_{ph} is measured between one line and the neutral, while line-to-line voltage V_{ll} is measured between two lines. The relation between phase and line-to-line voltage is

$$V_{ph} = \frac{V_{ll}}{\sqrt{3}}, \tag{4.1}$$

while the current flowing trough each line I_l is equal to the phase current I_{ph}

$$I_{ph} = I_l. \tag{4.2}$$

The three phase power is

$$P_s = 3R_s I_l^2 \tag{4.3}$$

where R_s is the per phase resistance.

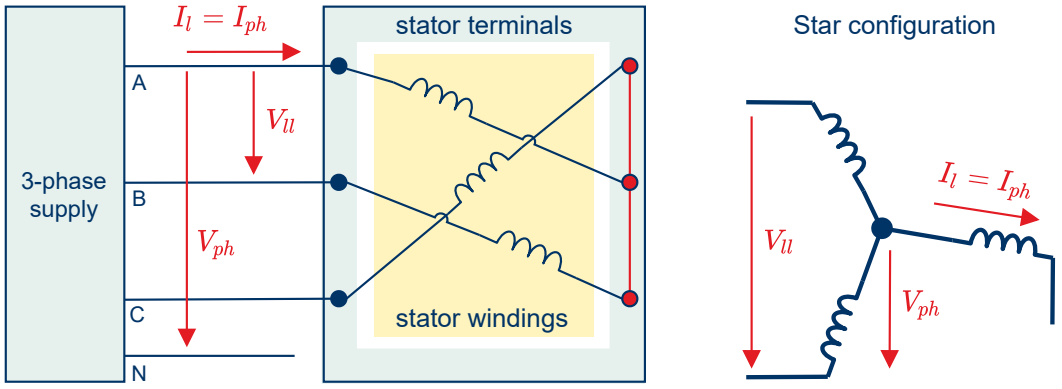

Figure 4.4: Star configuration

On the other hand, if the machine is delta connected, the configuration is shown in figure 4.5. Placing the measuring equipment the same way that in the previous configuration, the measurements taken are not the same, that is, the quantities being measured do not have the same meaning as before. Now, the line current I_l is not the phase current I_{ph}, since it is divided between two inductors of the stator winding. The relation between the two is

$$I_{ph} = \frac{I_l}{\sqrt{3}}. \tag{4.4}$$

The voltage between two lines is the phase voltage,

$$V_{ph} = V_{ll}, \tag{4.5}$$

since between two same side terminals, there is only one phase of the induction machine. The three

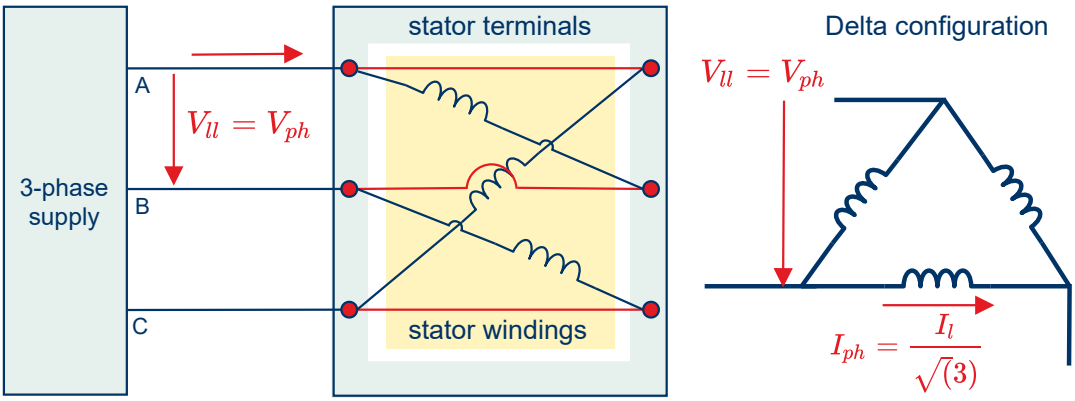

Figure 4.5: Delta configuration

phase power is

$$P_s = R_s I_l^2 \tag{4.6}$$

In several efficiency estimation methods, the stator resistance R_s is required. This reading is done directly with the motor connected in the configuration in which the tests are to be performed. The terminal resistance R_t is the average of the values of the terminal resistance measured in each pair of terminals (T1-T2, T1-T3, T3-T2). The relationship between the phase resistance and the terminal resistance is as follows, depending on the configuration of the stator windings

$$R_s = \frac{3}{2} R_{tDelta} \tag{4.7}$$

$$R_s = \frac{R_{tStar}}{2} \tag{4.8}$$

Chapter 5

Experimental Tests and Results

In this chapter, the experimental tests required for the several estimation methods are presented, as well as the obtained results. All data is taken with the machines working as a motor and the calculations done are only valid for this working condition.

The reference efficiency is calculated through a modified torque method, adjusted to use only readings that are possible in the laboratory, since torque sensors are not available. Because this is the most accurate value of efficiency that is possible to obtain, it is used as a reference. The rest of the methods are compared based on the absolute error between their efficiency curves and the reference efficiency curve.

Not all the estimation methods presented in chapter 2 were tested, since several of them require software or models that are not public or available. Hereupon, within the segregated losses methods, the IEEE std-112 Method B was tested and some approximations are presented in order to reduce its intrusiveness. The standard equivalent circuit is also calculated with several approximations. For the slip and current methods, six methods were tested, with different levels of intrusion and accuracy. The results are presented from the most intrusive estimation method to the less intrusive one.

5.1 Reference Efficiency

Since the focus of this study is to compare different efficiency estimation methods, namely its accuracy versus intrusiveness, there is the need to measure the true efficiency of the machine to use it as a reference. Since none of the machines is equipped with sensors that allow the direct measurement of their efficiency, indirect methods are used.

The efficiency of both machines is calculated by performing a load test and acquiring the input power P_s, the rotor speed N and the torque T. The rotor angular velocity ω_r is obtained from the rotor speed N by

$$\omega_r = \frac{2\,\pi}{60}\,N \tag{5.1}$$

and the useful mechanical power P_{mec} is calculated as follows

$$P_{mec} = T\omega_r. \tag{5.2}$$

The efficiency of both machines is calculated by

$$\eta = \frac{P_{mec}}{P_s} \times 100 \tag{5.3}$$

and plotted in figure 5.1.

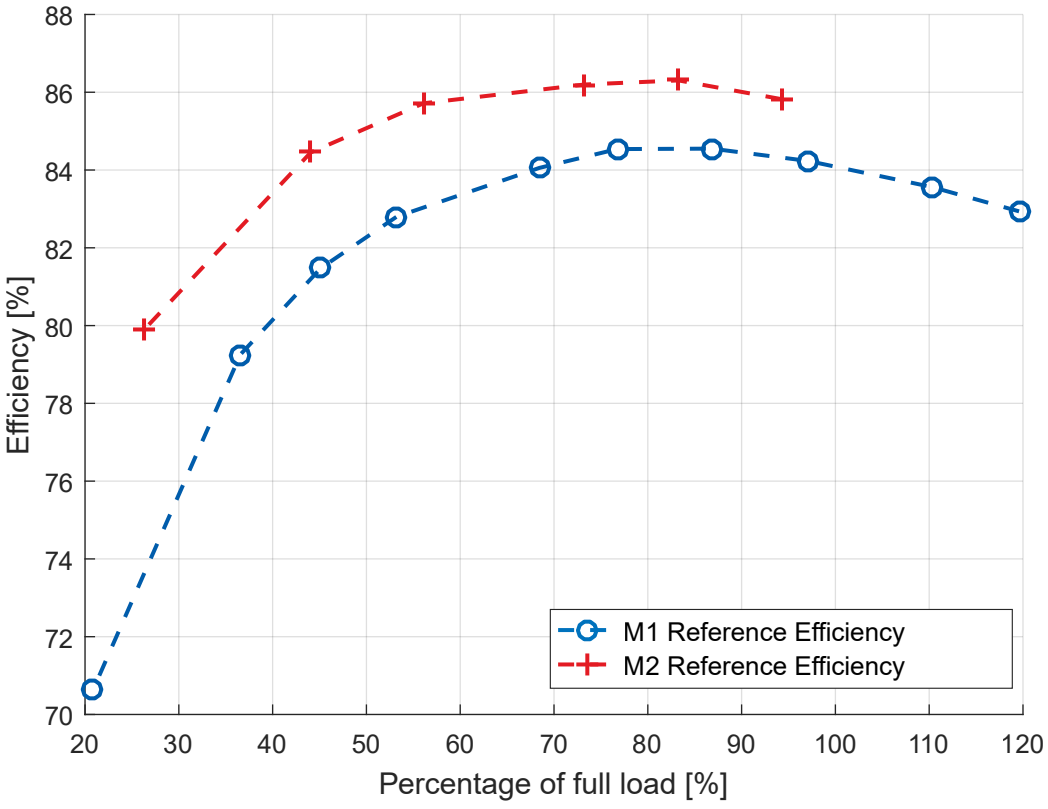

Figure 5.1: Efficiency curve of both machines

The IM2 efficiency curve has a smaller range of load points because of the current limitation of the resistive bank used to simulate the load.

Neither the machines is equipped with a torque sensor, so the torque is calculated indirectly in each of them. The DC machine coupled to IM1 is already studied from a previous thesis [14], where the torque coefficient K in (5.4) is obtained by a fitted function through several experimental tests.

$$K = -0.1355\ I_{exc}^4 + 0.8141\ I_{exc}^3 - 1.8403\ I_{exc}^2 + 1.9698\ I_{exc} - 0.0335 \tag{5.4}$$

Measuring the armature and excitation current, I_{arm} and I_{exc} respectively, it is possible to calculate the torque T produced by the machine

$$T = I_{arm}\ K, \tag{5.5}$$

admitting that the losses in the axis between the two machines are negligible.

The DC machine connected to IM2 has a movable stator, depicted in figure 5.2, making it possible to obtain the torque directly by placing weights in the plate on the end of the arm until it is balanced. Multiplying the weight by the gravitational acceleration and by the arm's length, the torque value is obtained.

Figure 5.2: DC machine with movable stator coupled to the 5.5 kW induction machine

5.2 Estimation Methods Results

5.2.1 Equivalent circuit

This method is highly intrusive since the tests needed require the machine to be taken out of service and uncoupled from its load.

Note that the no load readings are taken after the motor has been running long enough for the bearings to be properly lubricated, at rated voltage and frequency. In this case, the machine was kept running until its temperature stabilized. With the parameters obtained, it is possible to calculate the estimated efficiency of the machine.

The efficiency is calculated with (2) and plotted in figures 5.3 and 5.4 for two different values of stator resistance. The hot resistance is the value measured when the machine has been working for some time and is shut down, while the cold resistance is the value measured with the machine at ambient temperature. The error is a bit smaller for the hot resistance value, since the machine warms up with the increase of load.

Overall, this method is extremely accurate in both machines, having an error smaller than 3% in the worst case, and approximately 0.3% to 0.5% in the normal operating region of the induction machine (80% to 120% of full load), marked by the shaded area in both graphs.

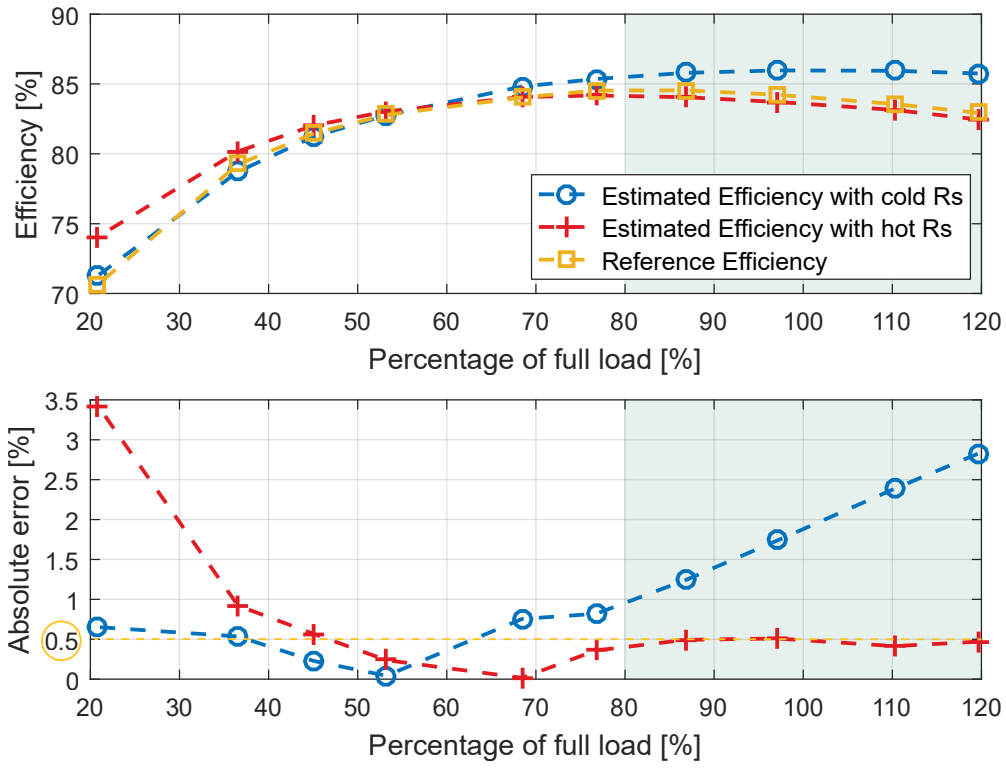

Figure 5.3: IM1 Efficiency curve obtained with the equivalent circuit estimation method

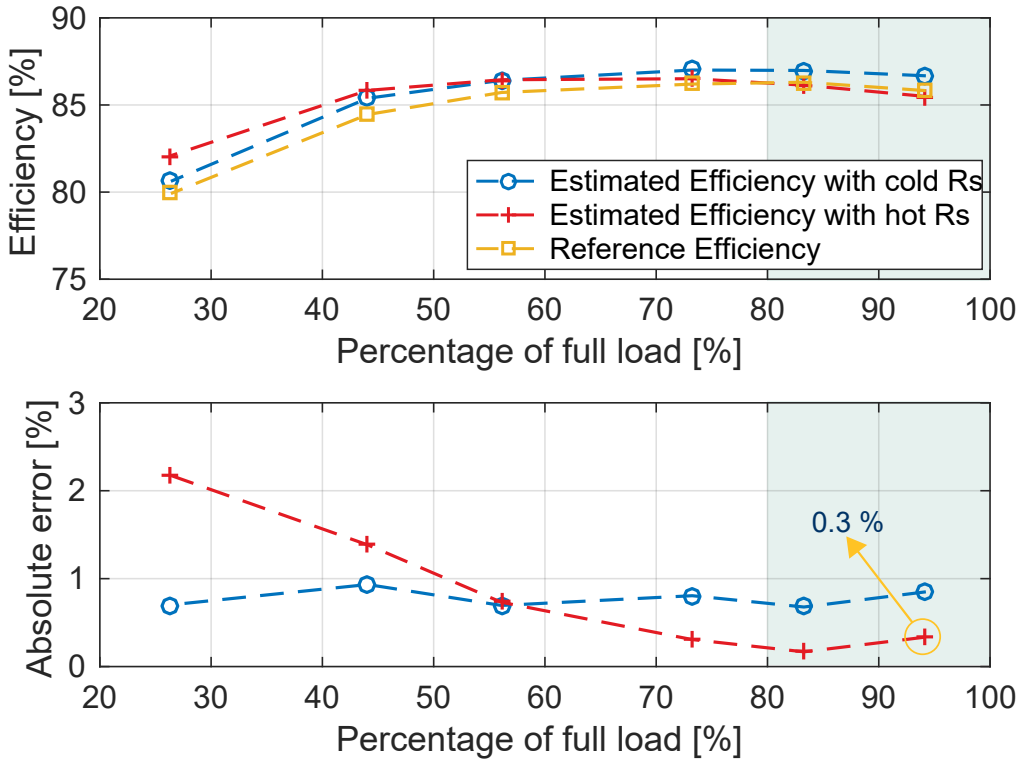

Figure 5.4: IM2 Efficiency curve obtained with the equivalent circuit estimation method

5.2.2 Method B IEEE Std.112

With a lower level of intrusion than the equivalent circuit method, is the IEEE Std-112 Method B, since it does not require a blocked rotor test. The purpose of this method is to calculate each type of loss individually to obtain the efficiency. It requires the acquisition of measurements at four different conditions: with the machine turned off, during the no load test, at rated load and in a range of several load points.

Cold Resistance

With the machine turned off and at ambient temperature, the stator resistance $R_{s\ cold}$ and the ambient temperature $T_{a\ cold}$ are measured.

Rated Load Test

The machine is loaded with rated load and the temperature of the stator is monitored until it reaches a stable value, that is, until it stops increasing. Since a temperature detector is not available in the motor, the outside temperature of the motor was monitored instead. When the stable point is achieved, the stator resistance $R_{s\ rl}$ and the ambient temperature $T_{amb\ rated}$ are measured. The stator windings temperature $T_{s\ rl}$ in this condition is calculated by,

$$T_{s\ rl} = \frac{R_{s\ rl}}{R_{s\ cold}}(k_1 + T_{a\ cold}) - k_1 \tag{5.6}$$

where k_1 is 234.5 for 100% IACS conductivity copper.

Load Test

The load test is performed to determine the stray-load loss. For this test the machine is subjected to several load points from 25 % of full load up to 150 %. Because of the current limitations of the machines and connected equipment, it is only possible to reach 120% of full load in IM1 and 95% in IM2. The stator resistance $R_{s\ load}$ is measured in each point after shutting down the machine as well as the ambient temperature $T_{amb\ load}$. The variables measured are line current I_{load}, phase voltage V_{load}, stator power P_{load}, power factor $cos(\phi)$, frequency f, rotor speed N_{load} and torque T in the case of IM2. The stator windings temperature $T_{s\ load}$ is calculated by (5.6), replacing the variables correspondent to the rated load test by the ones correspondent to the load test.

No Load Test

The no load test gives information about the core losses, windage and friction losses. This test is explained theoretically in section 3.3. For this, the machine must be ran with no coupled load and measurements are made between 120% of rated voltage down to the point where further decrease in voltage increases the current from the rated no-load current. Because of the current limitations in the machines and connected equipment, it is only possible to reach 115% of rated voltage for IM1 and 100%

for IM2. The stator resistance $R_{s\ nl}$ is measured in each point after shutting down the machine as well as the ambient temperature $T_{amb\ nl}$. The variables measured are line current I_{nl}, phase voltage V_{nl}, stator power P_{nl}, power factor $cos(\phi)$, grid electrical frequency f, rotor speed N_{nl}

Calculations and results

The calculations in this section refer to a star connected induction machine. In order to apply these equations to a delta connected machine, the modifications in section 4.2 need to be done.

The stator copper joule loss P_{sCu} is calculated for each point taken during the no load test by

$$P_{sCu} = 3I_{nl}^2 R_{s\ nl}. \tag{5.7}$$

As seen in section 3.2, the rest of the power loss is due to losses in the core and windage and friction,

$$P_C + P_{fw} = P_{nl} - P_{sCu}. \tag{5.8}$$

This power is plotted against the line-to-line squared voltage ($V_{ll} = \sqrt{3}\ V_{ph}$). To obtain the windage and friction value, the curve is extended to zero with a linear regression from the points of lower voltage. The windage and friction power loss P_{fw} is the interception with the zero voltage axis, for it is a constant loss. The voltage is squared in order to linearize the power curve. In figure 5.5 this procedure is represented for IM2.

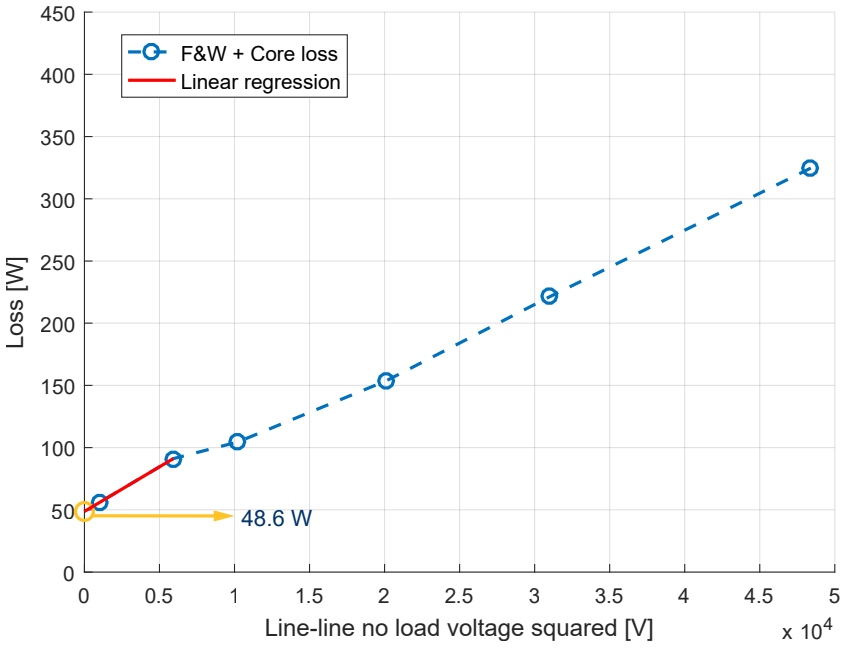

Figure 5.5: Extraction of friction and windage losses for IM2

The loss increases linearly with the squared voltage, since core losses are related to the square of the magnetic flux B, which is proportional to the square of the voltage. In figure 5.6, the exact same procedure is represented for IM1. Here, the friction and windage power loss reveals a non-linear evolution and reaches negative values.

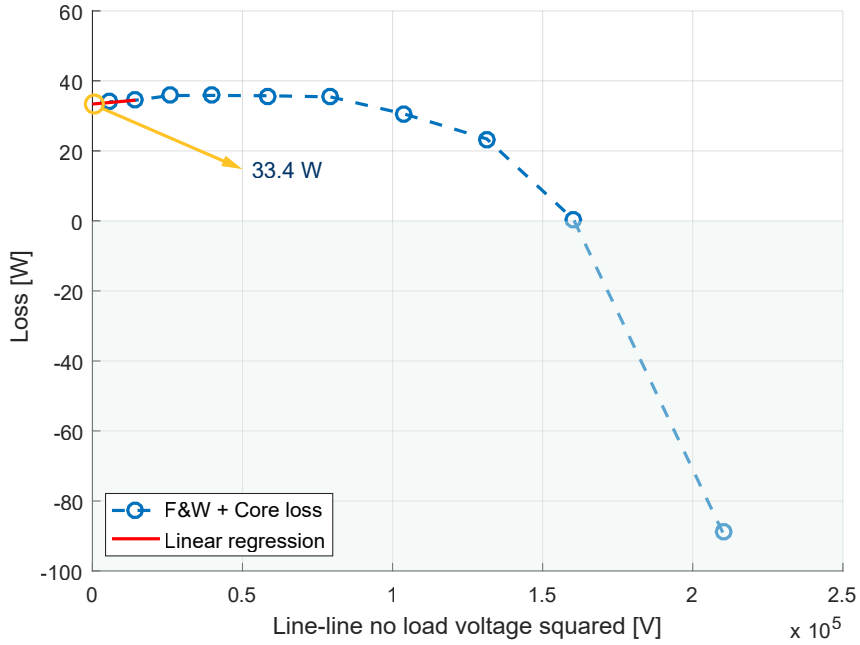

Figure 5.6: Extraction of friction and windage losses for IM1

This is not the expected behavior of this type of loss and is not considered accurate. Since the iron core of IM1 is smaller than IM2, the fluxes induced in the core are smaller, so joule losses become increasingly prevalent as the machine size decreases, not having enough precision to segregate the friction and windage losses. Therefore, the power plotted does not only represent the core and mechanical losses, but can also include eddy currents.

The next step is now to calculate the core losses, eddy currents and hysteresis losses. Since it is not possible to calculate the core loss precisely in IM1, it is considered null. This is going to influence the accuracy of the further efficiency estimations.

The core loss P_C can be calculated from the points taken in the no load test as follows

$$P_C = P_{nl} - P_{sCu} - P_{fw} \tag{5.9}$$

This power curve can be interpolated for the values of core voltage in the load condition to obtain the core loss, also in the load condition. The voltage drop in the iron core V_{core} is represented schematically in the equivalent circuit in figure 5.7.

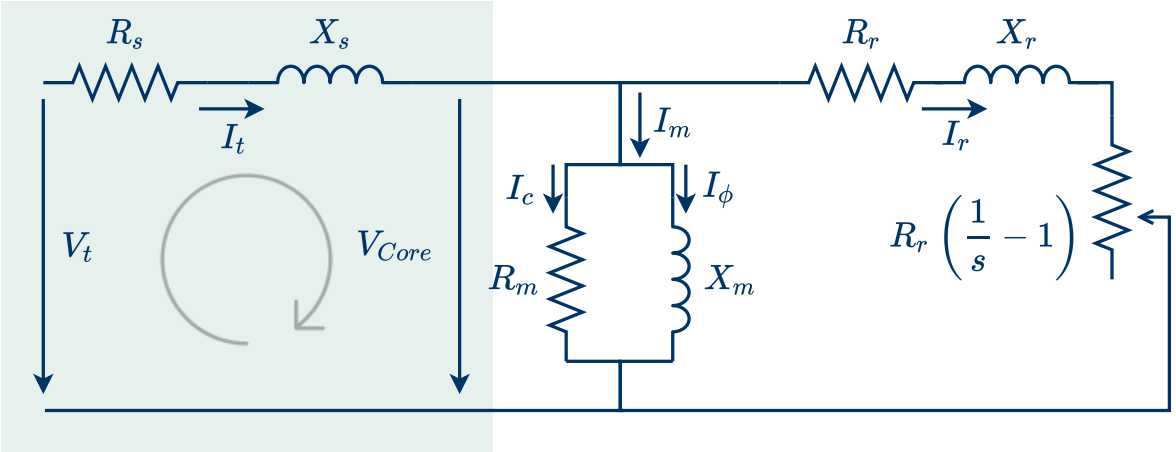

Figure 5.7: voltage drop in the core represented in the equivalent circuit of the induction machine

According to [1], the voltage drop across the stator leakage reactance is considered to be negligible. Focusing on the left loop of the equivalent circuit and neglecting the stator leakage reactance X_s, the circuit is simplified in figure 5.8.

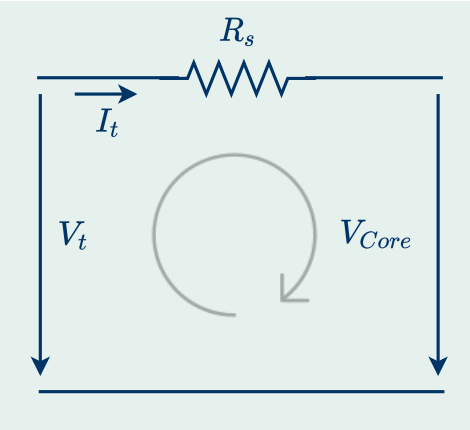

Figure 5.8: Simplified circuit for the core voltage calculation

The core voltage $\overline{V_{core}}$ is obtained by subtracting the resistive voltage drop in the stator winding from the terminal voltage $\overline{V_t}$ as follows,

$$\overline{V_{core}} = \overline{V_t} - \sqrt{3} I_t R_s. \tag{5.10}$$

where R_s is the stator winding resistance. Considering that the stator line-to-line voltage is of the form

$$\overline{V_t} = V_t e^{j0}, \tag{5.11}$$

the line current $\overline{I_t}$ is equal to

$$\overline{I_t} = I_t \cos\theta + j I_t \sin\theta. \tag{5.12}$$

Combining both equations, the following relation is obtained

$$V_t - \overline{V_{core}} = \sqrt{3} R_s I_t \cos\theta + j\sqrt{3} R_s I_t \sin\theta \tag{5.13}$$

and solving it for V_{core} one gets

$$V_{core} = \sqrt{(V_t - \sqrt{3}R_s I_t \cos\theta)^2 + (\sqrt{3}R_s I_t \sin\theta)^2} \tag{5.14}$$

since $PF = \cos\theta$, the equation to calculate V_{core} is deduced

$$V_{core} = \sqrt{(V_t - \sqrt{3}R_s I_t PF)^2 + (\sqrt{3}R_s I_t \sqrt{1 - PF^2})^2}. \tag{5.15}$$

The values of P_C in the the load condition are an interpolation of the values of the no load P_C obtained in (5.2.2) for the new values of V_{Core}. The core loss in the no load condition is plotted in blue in figure 5.9 and the interpolated values in red.

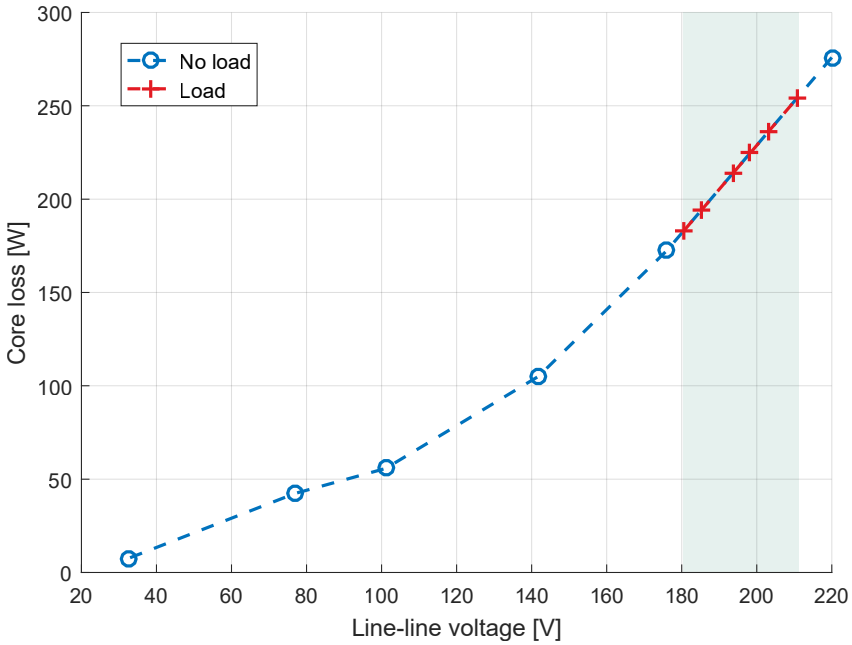

Figure 5.9: Core power loss interpolation for IM2

In the load condition, the joule losses are different from those calculated in the no load condition, since this losses are not fixed. The stator joule losses are calculated by

$$P_{sCu} = 3I_{load}^2 R_{s\ load}. \tag{5.16}$$

The power across the air gap P_{ag} is the sum of the losses in the iron and the copper losses in the stator subtracted from the input power

$$P_{ag} = P_{load} - P_C - P_{sCu}. \tag{5.17}$$

Since the rotor resistance R_r depends on slip, as it is explained in section 3.3, the rotor joule loss is calculated by

$$P_{rCu} = P_{ag} s_{load}. \tag{5.18}$$

where s_{load} is the value of slip during the load test.

This way, the total conventional loss is the sum of all the fixed and variable losses calculated,

$$P_{conv} = P_C + P_{sCu} + P_{rCu} + P_{fw}. \tag{5.19}$$

With the torque obtained from the DC machines, it is possible to calculate the mechanical power with (5.2). Subtracting this power from the input power, one obtains the apparent total loss P_{ap}.

The stray load losses are calculated as follows

$$P_{sl} = P_{ap} - P_{conv} \tag{5.20}$$

since they correspond to the rest of the power that is not due to the losses already calculated.

Because the core losses were considered null for IM1, due to the lack of precision in the estimations, the stray load losses value used in the calculations is the standardized one in table 5.1 [1], for a 0.7457 kW to 90 kW machine.

Table 5.1: Assumed values for stray-load loss

Machine rating (kW)	Stray-load loss percent of rated load
0.7457 to 90	1.8%
91 to 375	1.5%
376 to 1850	1.2%
1851 and greater	0.9%

To confirm the results of the stray load losses calculated for IM2, these losses are plotted as a function of the square of the load torque in figure 5.10. If the slope were to be negative, the results would be inconclusive, which is not the case.

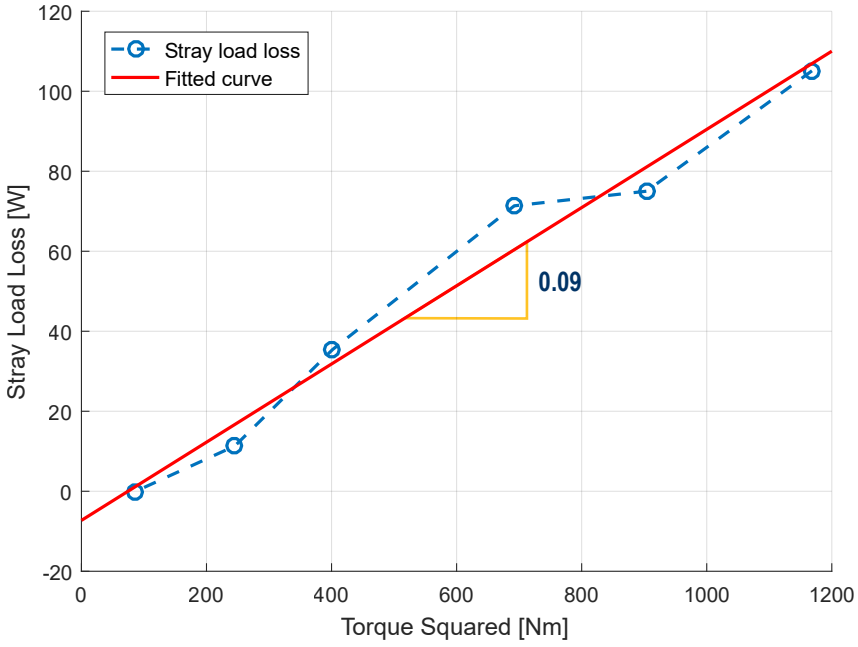

Figure 5.10: Stray load losses plotted against squared torque

Finally, the calculations are corrected to a reference ambient temperature of 25ºC. This is done because the resistances change with temperature, so all the variables that vary with resistances are corrected to a standard value of 25ºC. For that, the temperature rise of the stator windings T_{rise} is calculated by subtracting the ambient temperature during the load test $T_{amb\ load}$ from the temperature of the stator windings $T_{s\ load}$

$$T_{rise} = T_{s\ load} - T_{amb\ load}, \tag{5.21}$$

so the corrected temperature T_{s0}, is the amount of temperature rise between the cold machine and the machine after working at rated load for some time. This value is summed to the reference temperature in order to simulate the case where the test is done at 25ºC of ambient temperature and that the machine will increase its temperature equally independent of the initial ambient temperature

$$T_{s0} = T_{rise} + 25. \tag{5.22}$$

The resistance and slip are corrected to the new ambient temperature as follows:

$$R_{s\ corr} = R_{s\ rated}\frac{k_1 + T_{s0}}{k_1 + T_{s\ rl}} \tag{5.23}$$

$$s_{corr} = s_{load}\frac{k_1 + T_{s0}}{k_1 + T_{s\ load}} \tag{5.24}$$

where $k1$ is 234.5 for 100% IACS conductivity copper.

The resistance and slip dependent calculations are corrected for these new values, namely the stator joule loss

$$P_{sCu\ corr} = 3I_{load}^2 R_{s\ corr}, \tag{5.25}$$

the power across the air gap

$$P_{ag\ corr} = P_{load} - P_C - P_{sCu\ corr}, \tag{5.26}$$

the speed

$$N_{corr} = N_{load}(1 - s_{corr}), \tag{5.27}$$

and rotor joule loss

$$P_{rCu\ corr} = P_{ag\ corr} s_{corr}. \tag{5.28}$$

Thus, the corrected total loss is the sum of all the variable and constant losses:

$$P_{total\ loss} = P_C + P_{fw} + P_{sCu} + P_{rCu\ corr} + P_{sl}. \tag{5.29}$$

Since it was possible to segregate all the losses for IM2, their contribution to the total power loss is represented in figure 5.11 for the different load points.

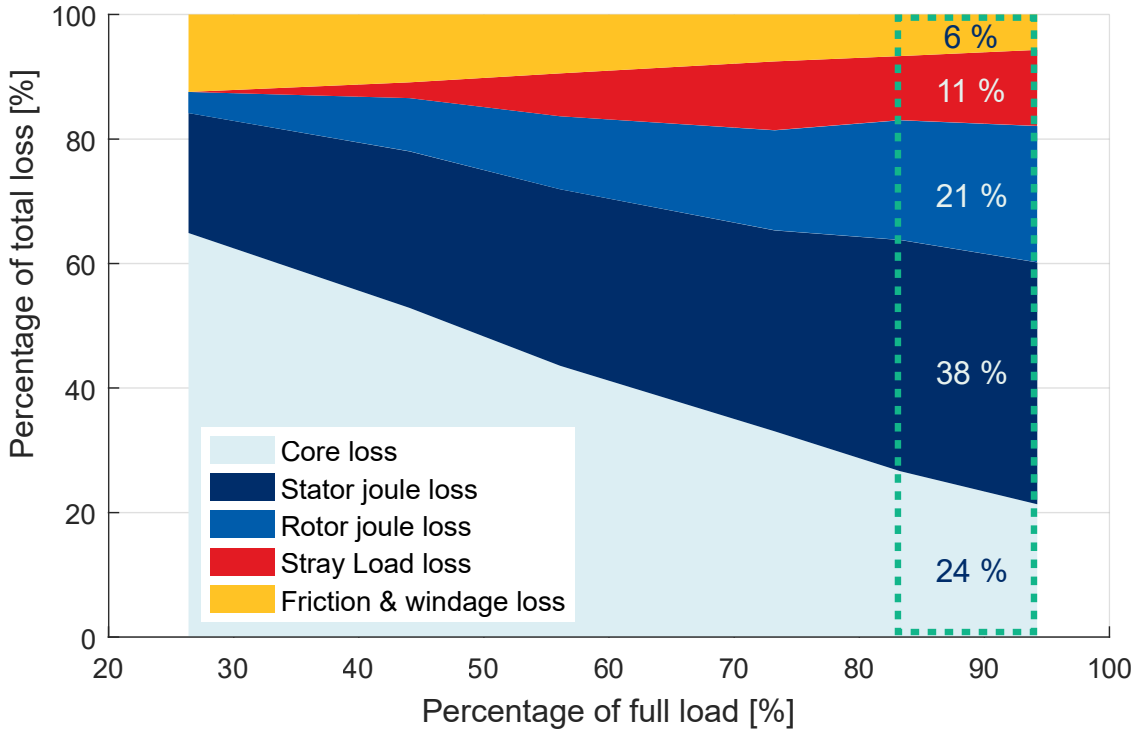

Figure 5.11: Induction Machine segregated losses percentage of total loss

The highlighted zone is the normal operation region in which stator joule losses contribute the most. It can also be noted that for higher loads, the core loss becomes less relevant while the joule losses prevail. The stray load losses also increase and the friction and windage loss, which is constant for all load points, has a decreasing contribution to the total loss. This way, the efficiency is calculated by

$$\eta = \frac{P_{load} - P_{total\ loss}}{P_{load}} \times 100 \tag{5.30}$$

The efficiency curve and the difference between the estimated and reference efficiency curves of IM1 are obtained and depicted in figure 5.12.

The results are very satisfactory since with a less intrusive method, the absolute error is kept under 3% in the normal operating region, shaded in blue. It is also emphasized how small the difference is, around 0.2%, between the values corrected to a 25ºC temperature and the values without the correction. Depending on the conditions of the testing, if the extra readings needed to correct the values mean more intrusiveness, then not performing this correction should be considered, for it does not increase the accuracy of the estimation considerably.

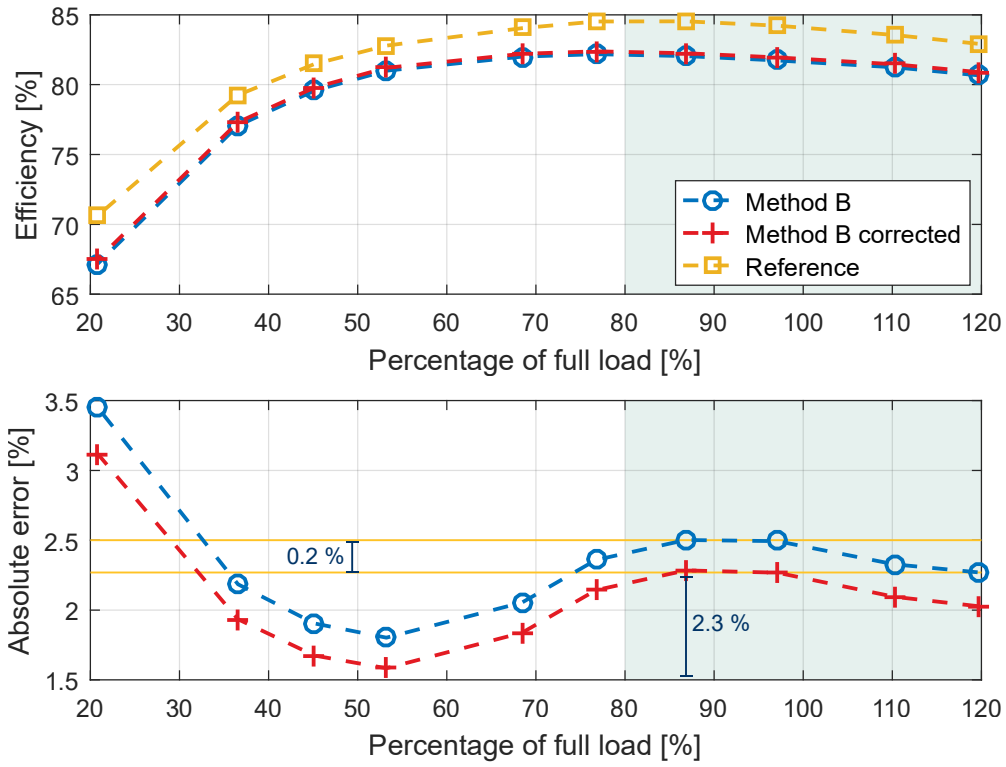

Figure 5.12: IM1 Efficiency curve obtained with Method B

As expected, the results in figure 5.13 obtained with the same method for IM2 are even better. Since all the losses were successfully segregated and there was no need to assume standardized values for some losses, the estimation is extremely precise, with an error very close to zero. On the point of lowest load, the stray load losses calculation become imprecise and have a negative value. This loss is assumed to be zero, which causes the error to rise as seen in figure 5.13.

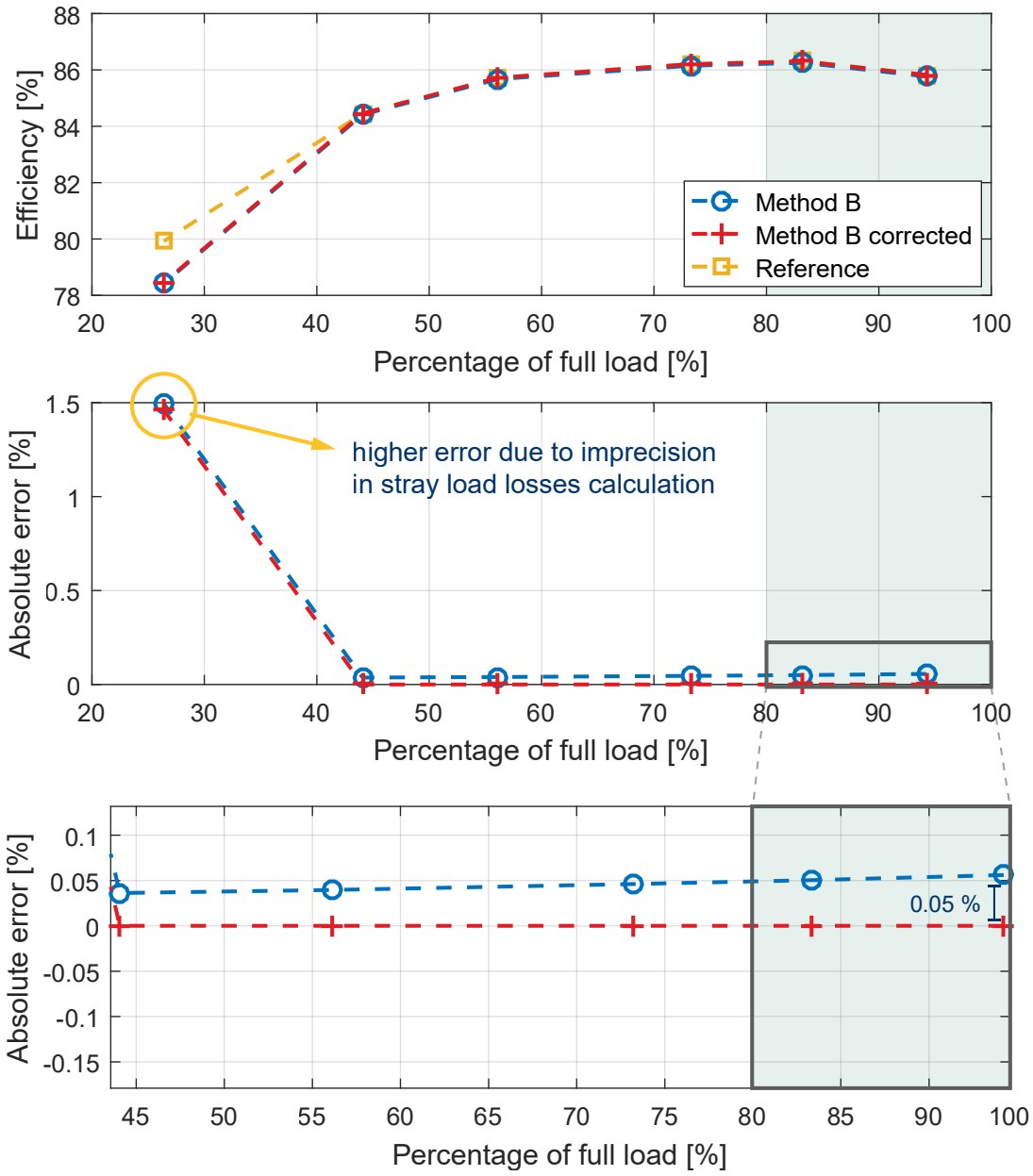

Figure 5.13: IM2 Efficiency curve obtained with Method B

5.2.3 Current Methods

Three current methods were tested in this experiment. The standard current method (Curr. method 1) is the simplest one, requiring only the current and power readings. The second method (Curr. method 2) is a corrected version of the first one that takes into account the offset of the current load curve by subtracting the no load current. The second method is expected to underestimate the efficiency so the third method (Curr. method 3) is the average of the first and second method and is supposed to increase the accuracy.

These characteristics are indeed observed when performing the estimation test on the bigger machine IM2 in figure 5.14. Current method 3 gives an efficiency estimation very close to the reference one, with an error of less than 2% on the normal operation region shaded in blue.

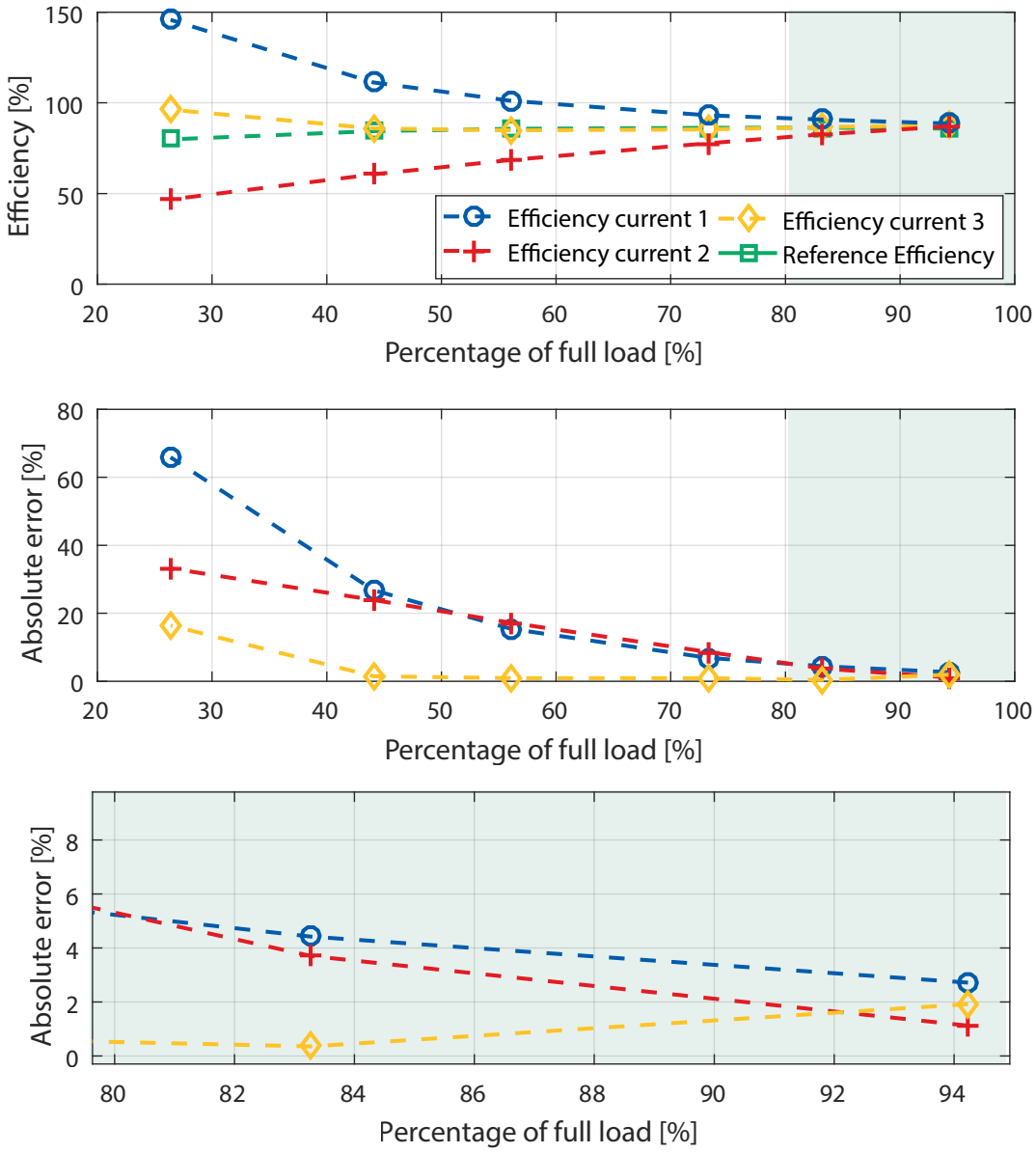

Figure 5.14: Current estimation method efficiency curve and absolute error for IM2

On the other hand, current method 1 turns out to be the most accurate in estimating the efficiency for the smaller machine IM1, showing a decrease in the absolute error of 7% to 2% between 95% to 120% of full load. This curves can be seen in figure 5.15. In this machine the estimations do not have the expected behavior. since the machine is smaller and precision errors start to become more relevant.

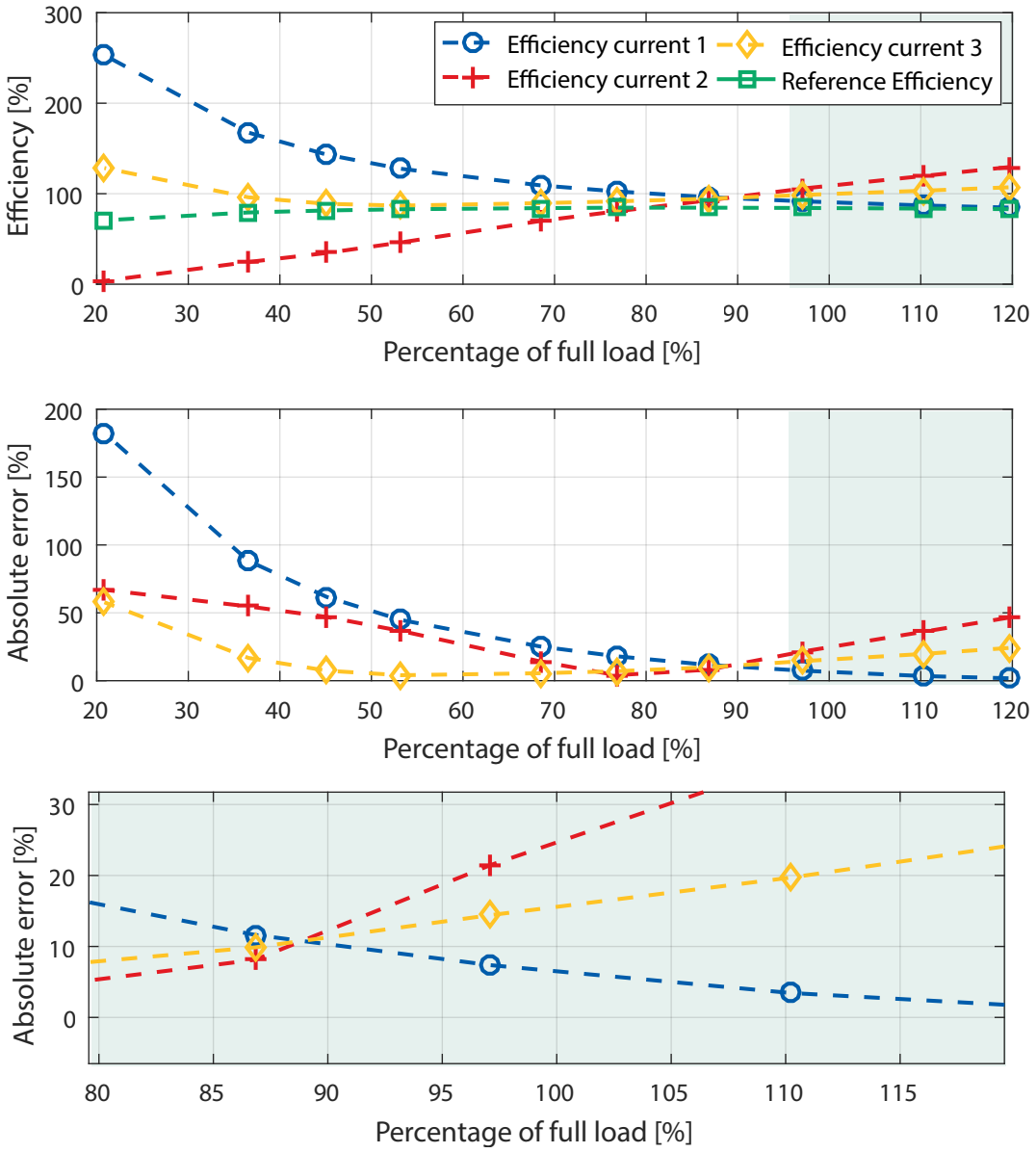

Figure 5.15: Current estimation method efficiency curve and absolute error for IM1

5.2.4 Slip Methods

The standard slip method (Slip method 1) is very simple and the readings required are the input power and rotor speed. The Ontario Hydro method (Slip method 2) is a variation of method 1 that corrects the rated nameplate speed for voltage variations, improving the accuracy in the shaded region near the full load point by 1% to 2% in both machines. Both curves are depicted in figures 5.16 and 5.17.

With the third method (Slip method 3), a considerably increase in accuracy is observed near the full load point, with an absolute error of approximately 1% in IM1 and 3% in IM2. With this increase in accuracy comes a higher intrusiveness, since this method requires additional measurements of stator resistance and current.

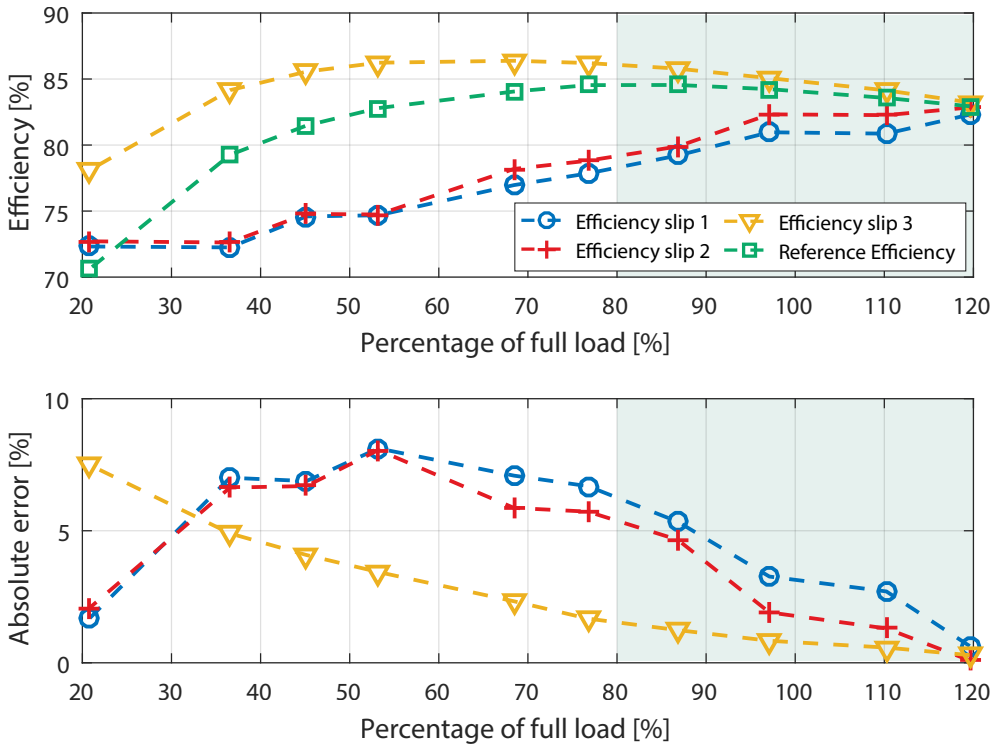

Figure 5.16: Slip estimation method efficiency curve and absolute error for IM1

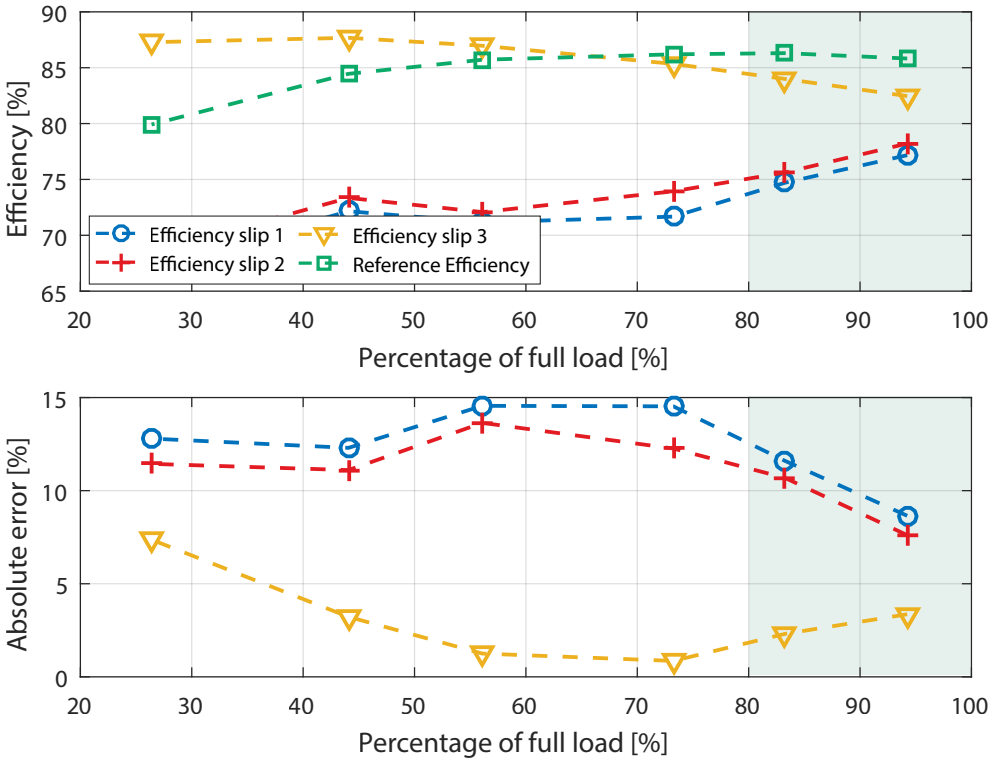

Figure 5.17: Slip estimation method efficiency curve and absolute error for IM2

5.2.5 Nameplate Method

The nameplate method is the less intrusive of all the methods studied since it only requires the nameplate data. The nameplate data is relative to one load point only, the rated or full load point. This way, the accuracy of this method is very dependent on the type of motor and on how much flat its efficiency curve is. As seen in figure 5.18, both efficiency curves are considerably flat, and IM2 has variation of efficiency of only 0.5% between 60% and 95% of full load.

These type of curves lead to a very small difference between the reference and estimated efficiency curves, even getting more accurate than other more intrusive methods. The efficiency curves and its absolute error for both machines can be observed in figure 5.19 and 5.20.

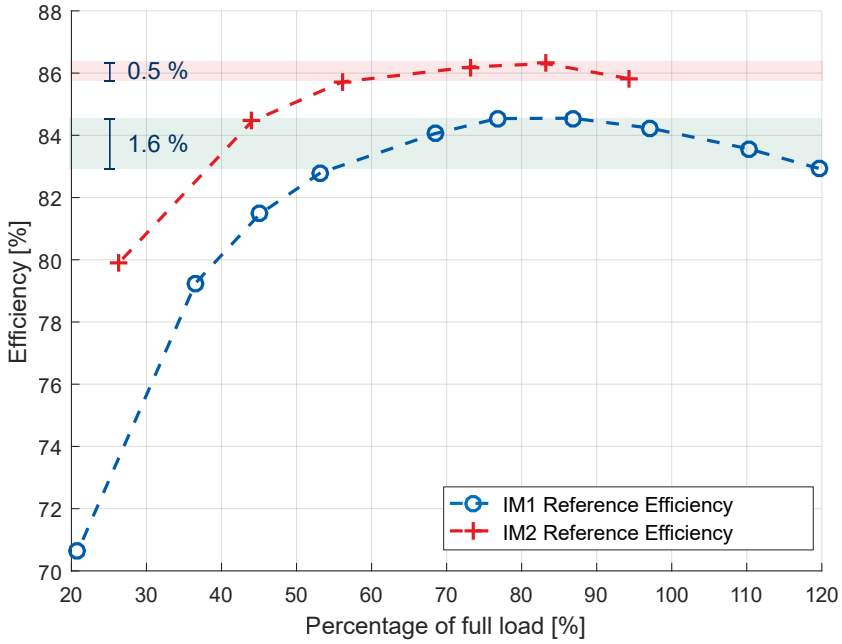

Figure 5.18: Induction Machines efficiency load curves

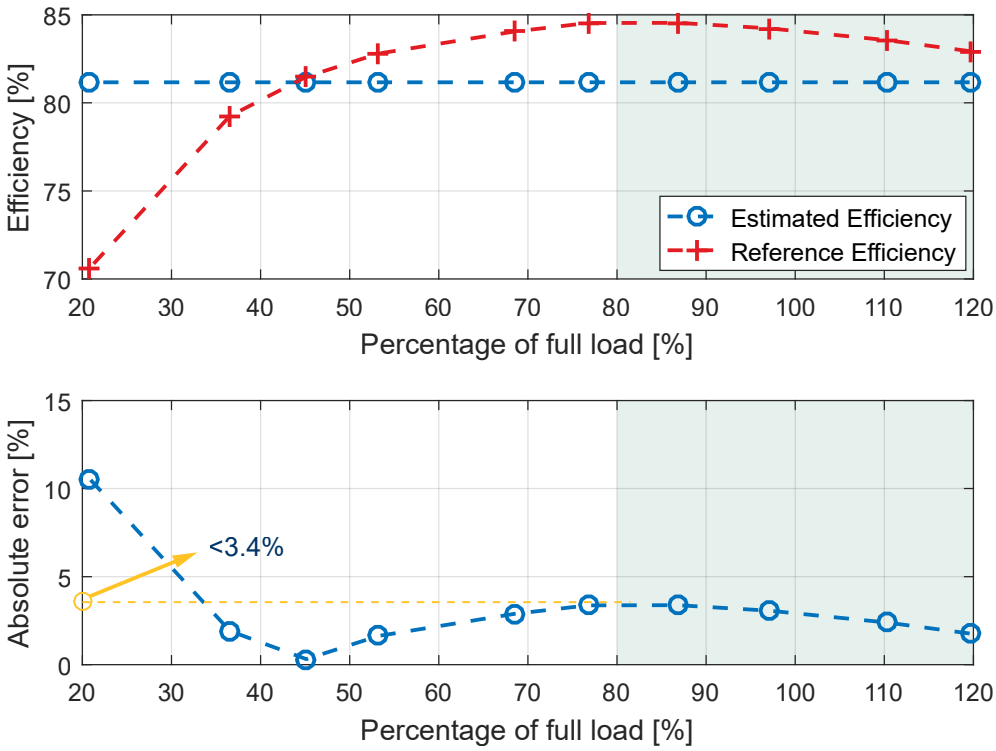

Figure 5.19: Nameplate estimation method efficiency curve and absolute error for IM1

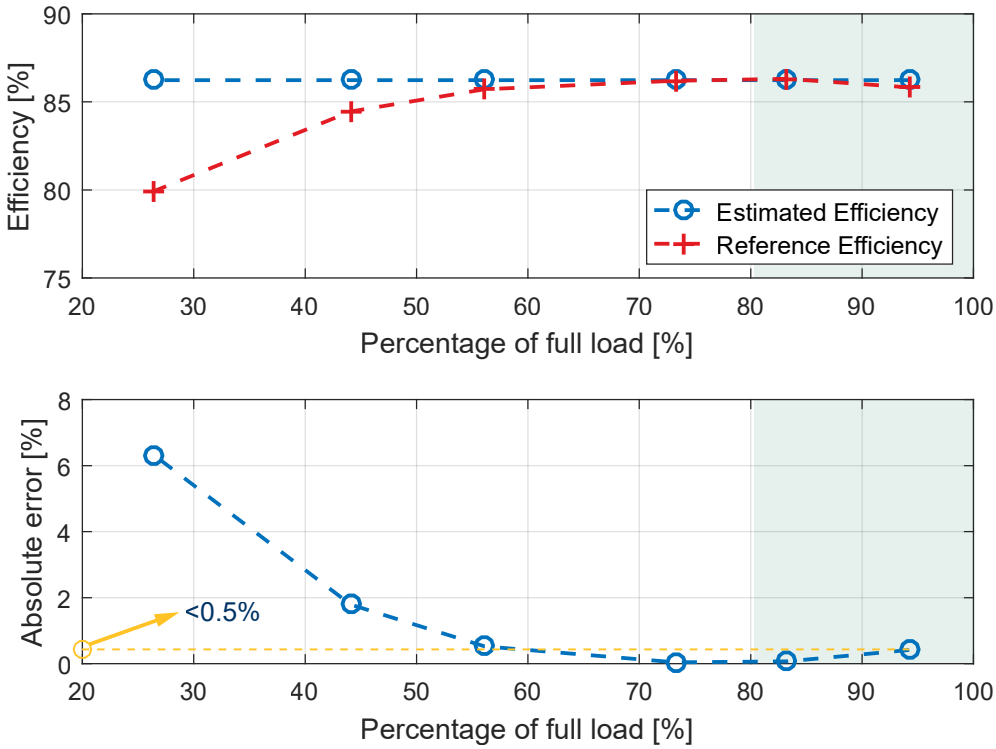

Figure 5.20: Nameplate estimation method efficiency curve and absolute error for IM2

5.2.6 Tests with connected inverter

The methods presented above are also applied to the same IM1 machine but with a connected inverter. As expected, the efficiency curve changes and can be seen in figure 5.21, next to the efficiency curve for IM1 without an inverter.

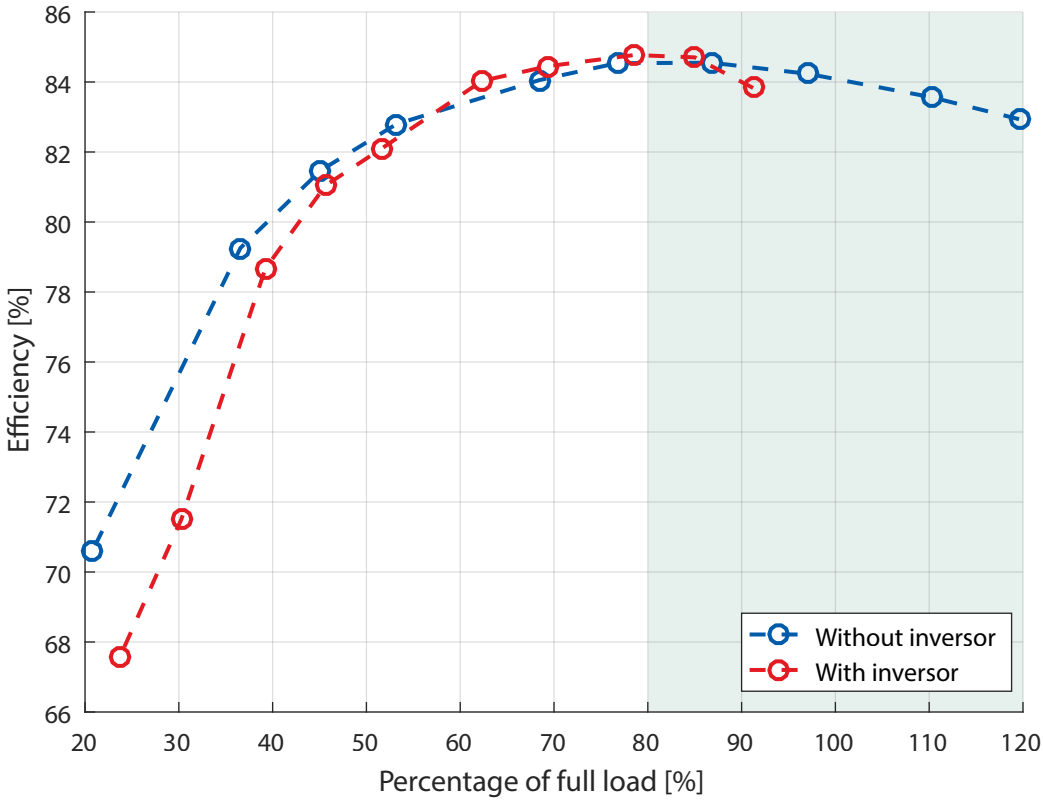

Figure 5.21: Efficiency curves for IM1 with and without a connected inverter

Fed by an inverter, the machine is subjected to an input voltage with harmonic content. Since the core loss varies with frequency, this type of loss increases and the efficiency drops slightly. The waveforms with and without the inverter are shown in figure 5.22, where it is possible to observe the noise added by the inverter.

This behavior, naturally affects the accuracy of the estimation methods. In figure **??** and 5.23b, the absolute error of each curve obtained with the efficiency estimation methods is compared.

Overall, the methods accuracy drops by a small percentage but the shape of the curves is similar to the ones obtained without an inverter. The nameplate method, the equivalent circuit method and the Method B estimated curves, all keep their absolute error below 4% in between 80% and 90% of full load.

On the other hand, the estimation methods in figure 5.23b have a significantly decrease in their accuracy. The current method that had an error below 5% in the usual range of operation, with the inverter has an error from 5% to 10% in the best case. The slip method 3 has a satisfactory accuracy below 5% but is most intrusive slip method.

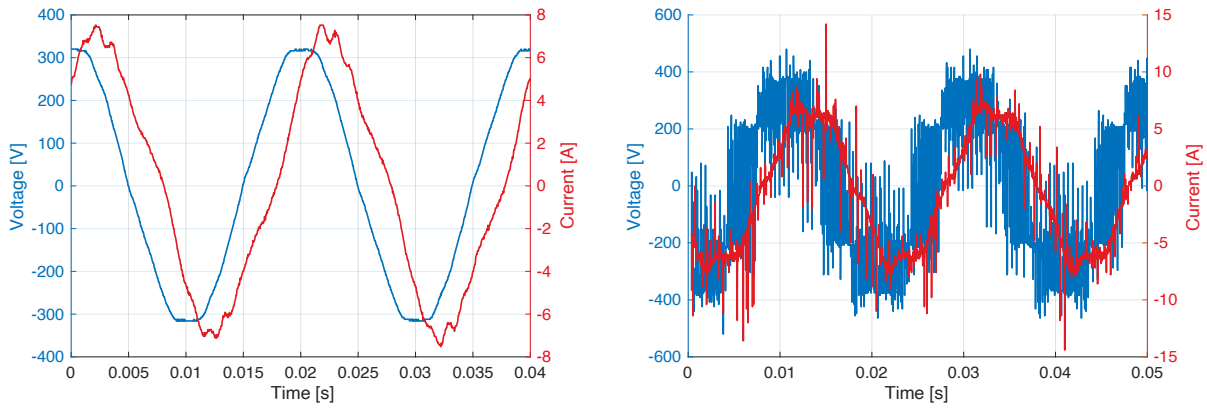

Figure 5.22: Voltage and current waveforms of the induction machine with and without a connected inverter

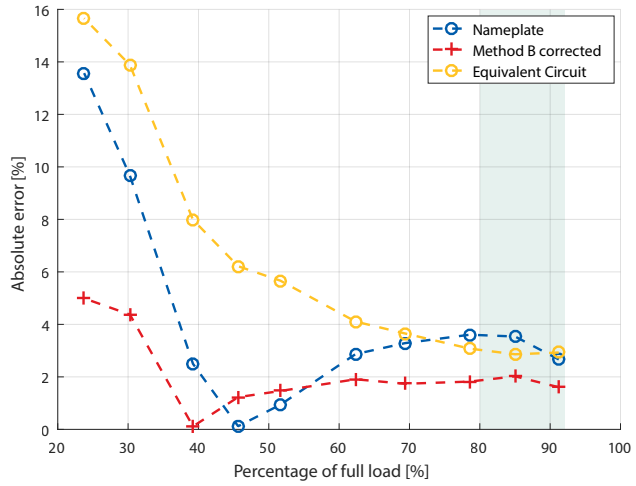

Figure 5.23: Efficiency estimation methods results for an inverter fed induction machine

Chapter 6

Conclusions

On chapter 5, it is possible to observe the differences between the estimation methods accuracy related to the intrusion level and the power of the machine. The achievements of the study are presented in section 6.1 by means of a table, comparing all the estimation methods accuracy and intrusion level. The future work is discussed in section 6.2, where possible paths for the continuation of this study are explored.

6.1 Achievements

The results of the efficiency estimation methods presented in section 5.2 are summarized in figure 6.1. On the left column, all the readings required for the several methods are presented: rotor speed (N), input voltage (V), input current (I), power factor (PF), stator resistance (Rs), mechanical torque (Torque), ambient temperature (Temp.) and nameplate data (NP). Following the parameters required, on the same column, are the tests required. On the first row of the table, all the methods tested are placed. The values in the table of the methods that require the stator resistance R_s, are done for a value of resistance measured are measured with the machine in a working temperature.

The last nine rows of the table, contain the maximum absolute error of each estimation in two intervals of percentage of full load. The first one, is the interval considered to be the usual range of percentage of load of a regular induction machine, the same used in chapter 5, that goes from 80% to 120% of full load, or in the case of IM2, up to 95% of full load, since it was not possible to reach higher values. The second range presented, is the interval where the accuracy is considered to be acceptable and can vary from the usual range. The errors are considered acceptable under 10%. This interval is considered for some methods have an high accuracy in regions outside the normal working zone, so could still be used in special applications where the machine is working on a specific range of full load.

Starting with the most intrusive methods, the Equivalent Circuit (Eq. circuit) and Method B (Meth.B). Both have low values of absolute error for both machines. The equivalent circuit has an error under 0.5% in both machines for ranges of load wider than the usual operating region. The estimation using Method B has outstanding results for IM2 but an absolute error of 2.3% for IM1. This is due to the incapability of measuring the core losses in a the smaller machine, so applying this method for machines smaller than IM2 might not be most adequate. This imprecision in measuring the losses can also be improved by using more precise measuring instruments.

The current methods, on the other hand, represent the worst values of accuracy. In the smaller machine IM1, the values of absolute error are considerably higher comparing to the ones of IM2. This result suggests that the current methods are more suited for bigger machines. The current method 3 is supposed to be the most accurate, since it represents the average between the overestimation of method 1 and the underestimation of method 2. However, for its low level of intrusion, the current method 1 presents a good accuracy, under 6% of absolute error, for the bigger machine and should be considered. In the other two methods the intrusion level rises with the need of performing the no load test.

In the case of slip methods, the absolute error appears to be higher for IM2 comparing with IM1. Slip method 3 is the most accurate and the rise in intrusiveness is low, since the stator terminals are usually exposed making it possible to measure the stator resistance R_s.

Finally, the nameplate method has incredible results with an absolute error of 0.4% in IM2 for the normal working region and even being able to guarantee an absolute error under 0.5% from half to full load. This is mainly due to the flat shape of both efficiency curves. To be noted that the motors tested are not new and are subjected to several undesirable conditions, since they are used by students in classes.

		Eq. circuit	Meth. B	Curr. 1	Curr. 2	Curr. 3	Slip 1	Slip 2	Slip 3	NP
Parameters requiered	N	x	x				x	x	x	
	V	x	x	x	x	x	x	x	x	
	I	x	x	x	x	x	x	x	x	
	PF	x	x	x	x	x	x	x	x	
	Rs	x	x						x	
	Torque		x							
	Temp.		x							
	NP	x	x	x	x	x	x	x		x
Tests	No load	x	x		x	x				
	Rated load		x							
	Locked rotor	x								
IM1	Max error usual range [%]	**0.5**	**2.3**	**16**	**46**	**24**	**6**	**5**	**1.5**	**3**
	Acceptable range [%Load]	[50,120]	[30,120]	[95,120]	[75,90]	[45,90]	[95,120]	[95,120]	-	[45,120]
	Max error acceptable range [%]	**0.5**	**2.3**	**8**	**10**	**10**	**3**	**2**	**-**	**3**
IM1 + Inverter	MAX error in usual range [%]	**3**	**2**	**16**	**16**	**14**	**13**	**12**	**1.4**	**3.5**
	Acceptable range [%Load]	[60,90]	[40,90]	-	[50,80]	-	90	90	[65,90]	[45,90]
	Max error acceptable range [%]	**4**	**2**	**-**	**7**	**-**	**3**	**3**	**2**	**3.5**
IM2	Max error in usual range [%]	**0.3**	**0.05**	**6**	**6**	**2**	**12**	**11**	**3**	**0.4**
	Acceptable range [%Load]	[70,95]	[45,95]	[86,95]	[83,95]	[45,95]	[90,95]	[90,95]	[60,95]	[55,95]
	Max error acceptable range [%]	**0.3**	**0.05**	**4**	**4**	**2**	**10**	**10**	**3**	**0.5**

Figure 6.1: Efficiency estimation methods comparison

The machine IM2 has more than 50 years old for instance, so even in this conditions the nameplate data is still accurate to estimate the efficiency with an error lower than 3%.

The efficiency estimations with a connected inverter are in general less accurate because of the harmonic content added. However, the current methods are considerably improved, since the efficiency is now lower for low loads, the methods improve in this region. Although the error is higher, the methods are still suited for an inverter-fed induction machine. This is an important result since in the industry, most induction machines are connected to electrical drives.

6.2 Future Work

The main improvement for a future continuation of this study is to test the methods in bigger machines. Most of the methods proved to be more accurate for IM2 and are probably better for even bigger machines.

The methods tested are the basis for more complex and precise methods and are the ones that are possible to perform with the material available. In order to test other methods or to improve the present ones, the measuring material could be improved, for instance, perform the tests with a torque sensor instead of using the torque coeffiecent of the DC machine in section 5.1.

Finally, with sensors and a microcontroller, this project could be transformed to estimate the efficiency of the machine in real time.

Bibliography

[1] Ieee standard test procedure for polyphase induction motors and generators. *IEEE Std 112-2017 (Revision of IEEE Std 112-2004)*, pages 1–115, 2018. doi: 10.1109/IEEESTD.2018.8291810.

[2] E. B. Agamloh. A comparison of direct and indirect measurement of induction motor efficiency. In *2009 IEEE International Electric Machines and Drives Conference*, pages 36–42, 2009. doi: 10.1109/IEMDC.2009.5075180.

[3] Bin Lu, T. G. Habetler, and R. G. Harley. A survey of efficiency-estimation methods for in-service induction motors. *IEEE Transactions on Industry Applications*, 42(4):924–933, 2006. doi: 10.1109/TIA.2006.876065.

[4] B. lu, T. Habetler, and R. Harley. A survey of efficiency estimation methods of in-service induction motors with considerations of condition monitoring requirements. pages 1365 – 1372, 06 2005. doi: 10.1109/IEMDC.2005.195900.

[5] N. E. M. Association. *Standard NEMA MG-1-1998: Motors and Generators*. Standard - National Electric Manufacturers Association. National Electrical Manufacturers Association, 2000. URL `https://books.google.pt/books?id=vNDdngEACAAJ`.

[6] Y. El-Ibiary. An accurate low-cost method for determining electric motors' efficiency for the purpose of plant energy management. *IEEE Transactions on Industry Applications*, 39(4):1205–1210, 2003. doi: 10.1109/TIA.2003.813686.

[7] J. S. Hsu, J. D. Kueck, M. Olszewski, D. A. Casada, P. J. Otaduy, and L. M. Tolbert. Comparison of induction motor field efficiency evaluation methods. *IEEE Transactions on Industry Applications*, 34(1):117–125, 1998. doi: 10.1109/28.658732.

[8] J. D. Kueck. Development of a method for estimating motor efficiency and analyzing motor condition. In *Conference Record of 1998 Annual Pulp and Paper Industry Technical Conference (Cat. No.98CH36219)*, pages 67–72, 1998. doi: 10.1109/PAPCON.1998.685505.

[9] B. Herndler. Non-intrusive efficiency estimation of induction machines. 2010.

[10] B. A. Nasir. An accurate iron core loss model in equivalent circuit of induction machines. *Journal of Energy*, 2020:7613737, Feb 2020. ISSN 2356-735X. doi: 10.1155/2020/7613737. URL `https://doi.org/10.1155/2020/7613737`.

[11] T. A. Lipo. *Calculation of Induction Machine Losses*, pages 193–250. 2018. doi: 10.1002/9781119352181.ch5.

[12] H. Kofler. Stray load losses in induction machines a review of experimental measuring methods and a critical performance evaluation. *Renewable Energy and Power Quality Journal*, 1:318–323, 04 2003. doi: 10.24084/repqj01.375.

[13] A. Fitzgerald, A. Fitzgerald, C. Kingsley, and S. Umans. *Electric Machinery*. McGraw-Hill higher education. McGraw-Hill, 2003. ISBN 9780073660097. URL `https://books.google.pt/books?id=teoeAQAAIAAJ`.

[14] J. P. R. F. Ferreira. Design and implementation of a current control system for a dc machine for emulation of linear and nonlinear mechanical loads in induction motors drives. Master's thesis, Instituto Superior Técnico, Universidade de Lisboa, Lisboa, Portugal, 2020. Unpublished.